4-86

SANDIA REPORT SAND84–1076 • Unlimited Release • UC–70
Printed October 1985

Nevada Nuclear Waste Storage Investigations Project

A Three-Dimensional Model of Reference Thermal/Mechanical and Hydrological Stratigraphy at Yucca Mountain, Southern Nevada

Terri S. Ortiz, Robert L. Williams, Francis B. Nimick,
Bruce C. Whittet, Don L. South

Prepared by
Sandia National Laboratories
Albuquerque, New Mexico 87185 and Livermore, California 94550
for the United States Department of Energy
under Contract DE-AC04-76DP00789

Distribution Category
UC-70

SAND84-1076

Unlimited Release
Printed October 1985

A THREE-DIMENSIONAL MODEL OF REFERENCE THERMAL/MECHANICAL AND HYDROLOGICAL STRATIGRAPHY AT YUCCA MOUNTAIN, SOUTHERN NEVADA

by

Terri S. Ortiz and
Robert L. Williams
Geoscience Analysis Division

Francis B. Nimick
NNWSI Geotechnical Projects Division

Bruce C. Whittet and
Don L. South
Geoscience Analysis Division

Sandia National Laboratories
Albuquerque, New Mexico 87185

ABSTRACT

The Nevada Nuclear Waste Storage Investigations (NNWSI) project is currently examining the feasibility of constructing a nuclear waste repository in the tuffs beneath Yucca Mountain. A three-dimensional model of the thermal/mechanical and hydrological reference stratigraphy at Yucca Mountain has been developed for use in performance assessment and repository design studies involving material properties data. The reference stratigraphy defines units with distinct thermal, physical, mechanical, and hydrological properties. The model is a collection of surface representations, each surface representing the base of a particular unit. The reliability of the model was evaluated by comparing the generated surfaces, existing geologic maps and cross sections, drill hole data, and geologic interpretation. Interpolation of surfaces between drill holes by the model closely matches the existing information. The top of a zone containing prevalent zeolites is defined and superimposed on the reference stratigraphy. Interpretation of the geometric relations between the zeolitic and thermal/mechanical and hydrological surfaces indicates that the zeolitic zone was established before the major portion of local fault displacement took place; however, faulting and zeolitization may have been partly concurrent. The thickness of the proposed repository host rock, the devitrified, relatively lithophysal-poor, moderately to densely welded portion of the Topopah Spring Member of the Paintbrush Tuff, was evaluated and varies from 400 to 800 ft in the repository area. The distance from the repository to groundwater level was estimated to vary from 700 to 1400 ft.

ACKNOWLEDGMENT

Our thanks are extended to John Lorenz and Dave Zeuch for their helpful review of this report.

CONTENTS

FIGURES

TABLES

INTRODUCTION

Yucca Mountain, located in and near the southwest corner of the Nevada Test Site (NTS) in southern Nye County, Nevada (Figure 1), has been identified by the Department of Energy (DOE) as a potential site for the disposal of radioactive waste. Responsibility for studying the suitability of Yucca Mountain as a disposal site rests with the Nevada Nuclear Waste Storage Investigations (NNWSI) Project, administered by the DOE offices in Las Vegas, Nevada. Sandia National Laboratories (SNL) is one of the primary NNWSI Project participants and has responsibilities for performance assessment, design, and rock testing. Information used in this report has also come from the U.S. Geological Survey, which is responsible for characterizing the geology and hydrology of the site, and from Los Alamos National Laboratory, which is responsible for characterizing the geochemistry of the site.

As part of its responsibilities, the NNWSI Project must determine whether a disposal site at Yucca Mountain satisfies Environmental Protection Agency (EPA) and Nuclear Regulatory Commission (NRC) criteria for geologic repositories. Such a determination requires an assessment of the radionuclide isolation capabilities of the site (performance assessment), which requires information on geology, geochemistry, hydrology, rock properties and design. Another essential activity within the NNWSI Project is that of repository design. Repository design also requires information on geology, geochemistry, hydrology, rock properties, and performance assessment. During construction, operation, and closure of an underground disposal facility, applicable mining and environmental safety standards must be satisfied.

Performance assessment and repository design activities require as input the characteristics and distribution of the rock units and geologic structures at Yucca Mountain. A previous report (Nimick and Williams, 1984, pp. 7-8) discussed the rationale behind this requirement as well as the initial stages in the implementation of a model that could provide the required input.

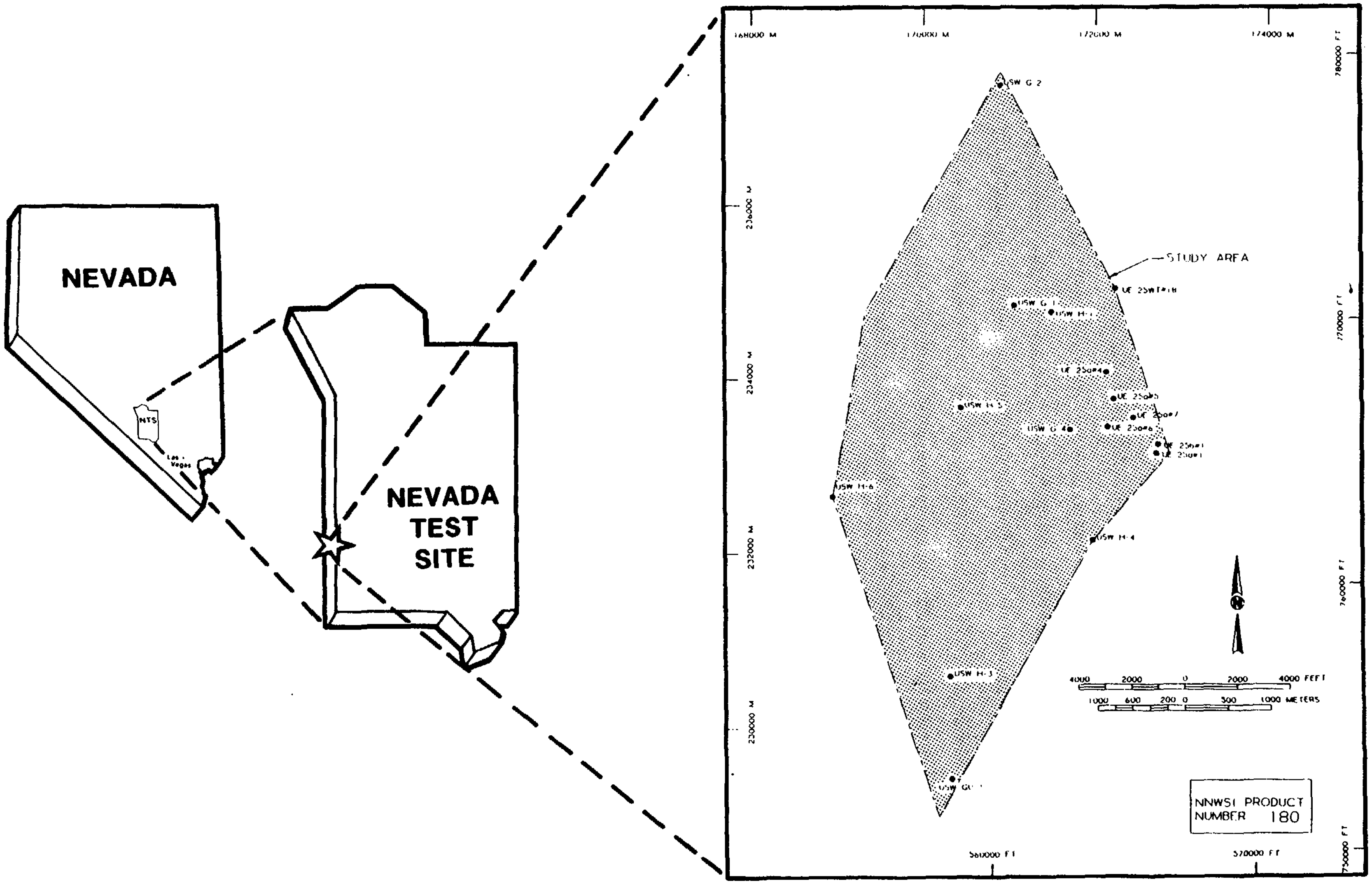

Figure 1. Location of area for which reference stratigraphy was modeled. Axis labels are Nevada state coordinates.

The previous work was performed using the geological stratigraphic units as a framework for three-dimensional geometric modeling. Unfortunately, such a division does not lend itself readily to describing the material properties because a formation may contain more than one type of rock. In fact, most formations at Yucca Mountain include at least two different types of tuff: welded ashflows and bedded tuffs.

The intent of this report is to provide a geometric representation of the rocks at Yucca Mountain, which, with associated material properties, can be used in performance assessment and repository design calculations. A stratigraphy based on porosity and grain density (Nimick, et al, 1984) that can be correlated to thermal, mechanical, and hydrological properties has been used in the model discussed in this report. In the future, a mineralogical and geochemical stratigraphy will be developed and modeled. At this time, only one mineralogical surface is included in the model.

This report will summarize the modeling technique used for the reference thermal/mechanical and hydrological stratigraphy and will describe the input data. The reliability of the reference stratigraphy will be evaluated and some surfaces important to repository design and performance assessment will be discussed. The report will conclude with a brief discussion about the uses for the model.

MODEL AND MODELING TECHNIQUE

The geometric model used for this work consists of a collection of three-dimensional surface representations--one surface for the base of each thermal/mechanical and hydrological reference unit. A three-dimensional interactive computer graphics system in the NNWSI Project Department at SNL was used to generate the model because of its data input, manipulation, and output capabilities. The graphics system, a computer-aided design (CAD) system, provides multiple methods of interactively viewing, measuring, and modifying three-dimensional line and grid data (Appendix A).

Field information concerning the nature and distribution of rock units at Yucca Mountain is limited to surface geologic maps and drill hole logs. However, a method of analytically interpolating among sparse and irregularly spaced data was developed at SNL (Williams and Nimick, in preparation) and was used for the earlier geologic model of Yucca Mountain (Nimick and Williams, 1984, pp. 8-10). The method generates a single, continuous analytical surface equation from a collection of three-dimensional coordinates. More specifically, a best-fit bias or trend surface is found, and then that trend surface is adjusted to pass exactly through the input points. An example of such an adjustment at an input point is shown in Figure 2. The technique and the reasons for its development will be documented in Williams and Nimick (in preparation), see also Nimick and Williams (1984, Appendix B).

The development of a three-dimensional model is shown schematically in Figure 3. Although input data from drill holes are too sparse to enable interpretation of the location of all faults, information on faults is available from surface mapping. Prefaulted coordinates of units were used as input data to give better results. Fault location, orientation, and relative displacement are used to transform coordinates obtained from drill holes for the bases of units to the coordinates of "prefaulted" units. A mathematical estimation technique (Williams and Nimick, in preparation, and Nimick and Williams, 1984, Appendix B) is then applied to the data, resulting in a set of

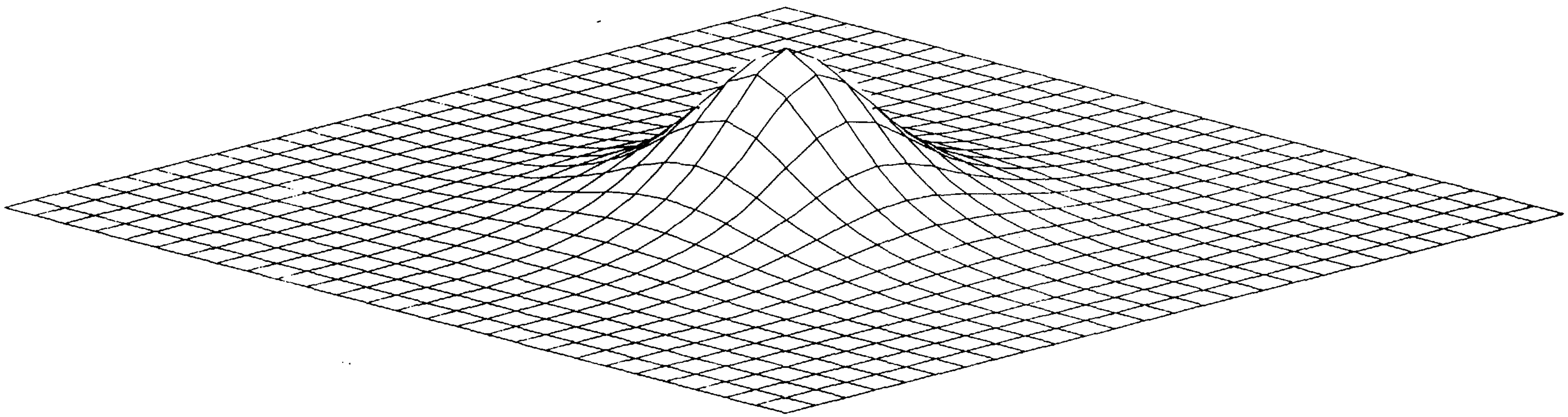

Figure 2. Example of surface adjustment at an input point (from Nimick and Williams, 1984, p. 60).

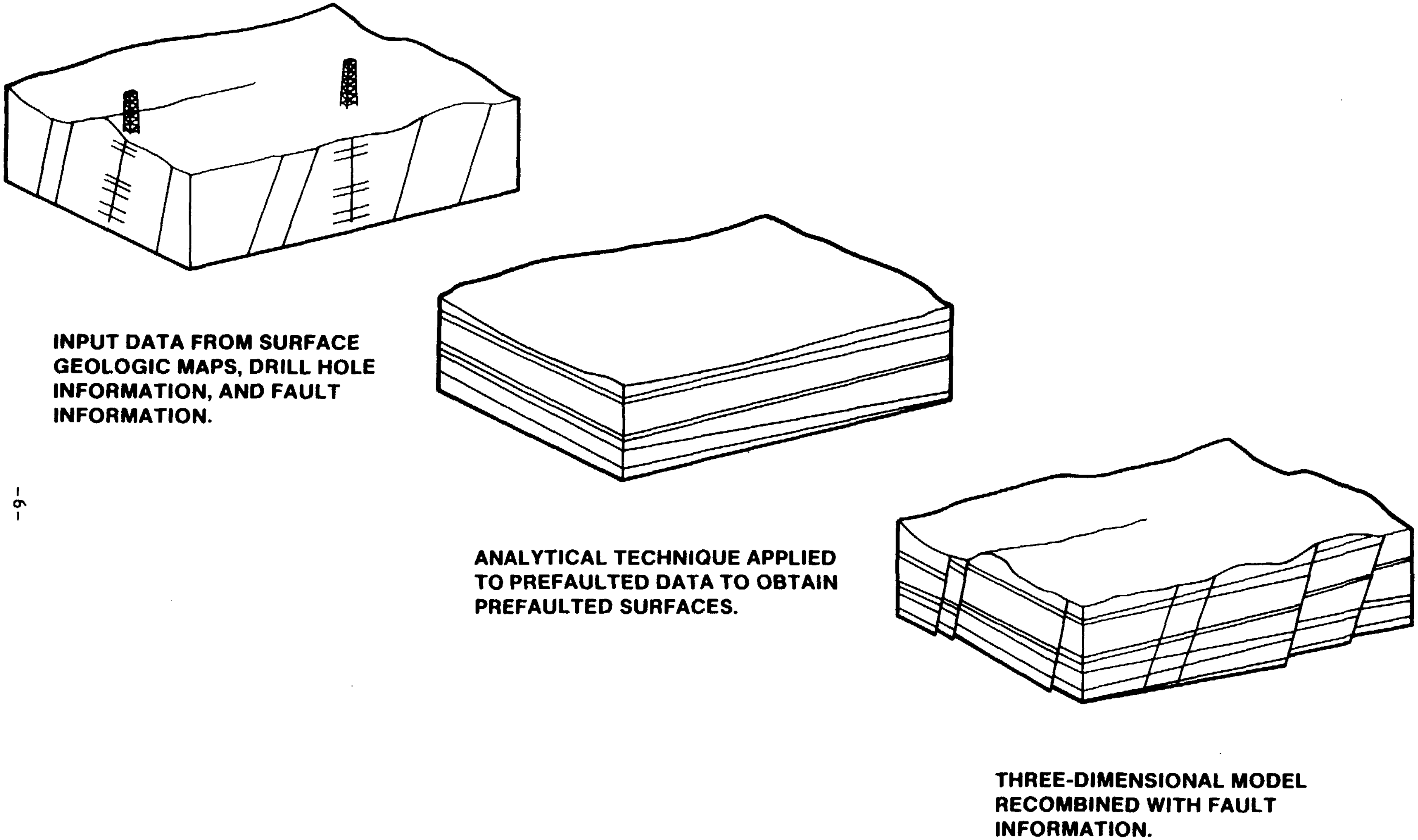

Figure 3. Schematic development of three-dimensional model.

analytical equations, each of which represents the base of a single defined unit. This set of equations and interactively recombined fault information comprise the major form of the model. The coefficients of the estimation equation, once generated, are stored on the graphics system and can be used in an interactive fashion to produce point, line, and grid data.

An assumption has been made that the actual surfaces were smooth and continuous when originally formed. The presence and effect of strong deviations from such a smooth surface (i.e., erosion features or igneous structures) cannot be assessed.

The previous three-dimensional model (Nimick and Williams, 1984) and the reference stratigraphy model both use planar trends. An attempt was made to select the best adjusted trend surface for a specific data set from all possibilities up to and including surfaces generated from 10-term cubic equations. A particular best-fit surface was selected by an evaluation of the ability of the surface to predict known data points that were not in the input data set. The surfaces selected by that method, which included quadratic and cubic terms, were mathematically plausible. However, away from data points, trends were skewed and not geologically reasonable. In all cases, planar trend surfaces produced the best results based on geological interpretation.

An assumption was made in the earlier three-dimensional modeling that the locations of stratigraphic pinchouts (locations where units have thinned to 0 ft) always occurred precisely at drill holes (Nimick and Williams, 1984, p. 15). For the reference stratigraphy model, locations of pinchouts are predicted by the model.

INPUT DATA

Yucca Mountain is a group of north-trending, fault-block ridges tilted gently eastward. In the study area (Figure 1), dips generally average 5 to 7 degrees except in the extreme southeast portion where dips up to 49 degrees occur (Scott and Bonk, 1984). Topography is controlled by high-angle, north-northeasterly striking major normal faults. Northwesterly trending strike-slip faults also occur. Minor normal faults and fractures are present within the blocks. The mountain is comprised of a 5000 to 13,000 ft sequence of silicic volcanic rocks of Tertiary age (Scott et al., 1983, pp. 290-292).

The concept of a stratigraphy for the Yucca Mountain tuffs based on rock properties rather than on classical geologic guidelines was first proposed by Lappin et al (1982, pp. 20-24). They used rock properties as the basis for defining a thermal stratigraphy in drill hole USW G-1. Subsequent analysis has indicated that the stratigraphy could be used with little modification for physical, mechanical and hydrological properties. The thermal/mechanical and hydrological reference stratigraphy evaluated in this report is an expansion and revision of the stratigraphy originally proposed solely for thermal properties by Lappin et al. Changes are the result of the availability of new information rather than from any change in the manner in which units are defined.

Two properties used to differentiate units are porosity and grain density. The following list indicates the general characteristics of these properties in each type of rock.

- Devitrified tuff: high grain density, low porosity.
- Vitric, welded tuff: low grain density, low porosity.
- Vitric, non-welded tuff: low grain density, high porosity.
- Zeolitized tuff: low grain density (higher than vitric), high porosity.

The adjectives "high" and "low" are relative terms without specific quantitative equivalents because each lithologic type has a range for each property, and the ranges frequently overlap.

Several types of data were used to define the contacts including lithologic logs, physical properties, X-ray analyses, and geophysical logs. Descriptions from the lithologic logs were most useful for distinguishing vitric and devitrified ashflows and bedded units. The definition of contacts between zeolitic units and nonzeolitic zones usually requires X-ray and/or physical property data. Geophysical logs were used only as a last resort because contacts between units with different mineralogies are often gradational and thus not readily distinquished on geophysical logs.

The locations of contacts interpreted from core were compared to selected geophysical logs. Information from that comparison was used to define similar characteristics in drill holes in which contacts were not previously defined. The most useful logs were the density and epithermal neutron porosity logs. As is the case with the physical properties, the usefulness of the geophysical logs varied from drill hole to drill hole.

The uncertainty associated with the location of contacts defined from lithologic logs is the error associated with depth assignment and lithologic interpretation during core logging operations and is, in general, quite small relative to other uncertainties. Thus, it is assumed that no error exists in contact depths picked from lithologic logs or in the depths of X-ray samples, physical property samples, or depths on geophysical logs because these last three measurements are all tied to the same measuring system as are the lithologic logs.

Uncertainties about the location of contacts defined using data from physical properties, X-ray analyses, and geophysical logs are provided in Appendix B where they could be estimated. The largest uncertainties are usually associated with contacts of zeolitized units with other lithologies.

Correlation of Units

Table 1 is a description of the reference stratigraphic units. In addition, zeolitic zones of Vaniman et al (1984) are included in Table 1. Elevations of the reference stratigraphic unit contacts and the criteria used in determining them in individual drill holes are provided in Appendix B. The correlation between the reference stratigraphy and the geologic stratigraphy is presented in Figure B-1.

Sixteen reference units have been defined. The undifferentiated overburden (UO) consists of any or all of the following geologic units: alluvium; colluvium; nonwelded, vitric portions of the Tiva Canyon Member of the Paintbrush Tuff; and any other tuff units that stratigraphically overlie the welded, devitrified Tiva Canyon Member. However, in core holes at Yucca Mountain used for this study, the overburden is represented only by alluvium in most cases. Because no data on rock properties have been obtained for these units from laboratory experiments, and because the overburden is commonly thin or nonexistent at Yucca Mountain, the overburden was not modeled. However, occurrences of alluvium are indicated by QTac where appropriate on figures. Where available, thicknesses of the overburden are indicated in Tables B-1 through B-12 in Appendix B.

In addition to the reference units, a mineralogical surface, TZZ, has been modeled that corresponds to the upper limit of prevalent zeolites. The distribution of zeolites does not correlate directly to stratigraphic units because zeolites have formed only in units that were susceptible to the alteration process. In general, tuffs that were originally vitric and porous (non- to partially welded) were zeolitized when they came in contact with groundwater for sufficient lengths of time. Generally, devitrified tuffs have been unaffected by the zeolitization.

Table 1
Description of Units

Description	Reference Stratigraphy Unit Name (Designator)	Zeolitic Zones of Vaniman et al., 1984
Alluvium; colluvium; nonwelded, vitric ashflow tuff of the Tiva Canyon Member of the Paintbrush Tuff; any other tuff units that stratigraphically overlie the welded, devitrified Tiva Canyon Member.	Undifferentiated Overburden (UO)	
Moderately to densely welded, devitrified ashflow tuff of the Tiva Canyon Member of the Paintbrush Tuff.	Tiva Canyon welded unit (TCw)	
Partially welded to nonwelded, vitric and occasionally devitrified tuffs of the lower Tiva Canyon, the Yucca Mountain, the Pah Canyon, and the Topopah Spring Members of the Paintbrush Tuff.	Upper Paintbrush nonwelded unit (PTn)	
Moderately to densely welded, devitrified ashflows of the Topopah Spring Member of the Paintbrush Tuff that locally contain more than approximately 10% by volume lithophysal cavities.	Topopah Spring welded unit, lithophysae-rich (TSw1)	
Moderately to densely welded, devitrified ashflows of the Topopah Spring Member of the Paintbrush Tuff that contain less than approximately 10% by volume lithophysal cavities. This is the proposed repository host rock.	Topopah Spring welded unit, lithophysae-poor (TSw2)	

Table 1 (Continued)
Description of Units

Description	Reference Stratigraphy Unit Name (Designator)	Zeolitic Zones of Vaniman et al., 1984
Vitrophyre near the base of the Topopah Spring Member of the Paintbrush Tuff.	Topopah Spring welded unit, vitrophyre (TSw3)	Interval I
Nonwelded ashflows, bedded and reworked tuffs of the lower Topopah Spring Member of the Paintbrush Tuff and the Tuffaceous Beds of Calico Hills.	Calico Hills and Lower Paintbrush nonwelded unit (CHn1)	Interval II
Basal bedded and reworked zones of the Tuffaceous Beds of the Calico Hills.	Calico Hills and Lower Paintbrush nonwelded unit (CHn2)	Interval II
Upper partially welded ashflows of the Prow Pass Member of the Crater Flat Tuff.	Calico Hills and Lower Paintbrush nonwelded unit (CHn3)	Interval II
Moderately welded, devitrified ashflows of the Prow Pass Member of the Crater Flat Tuff.	Prow Pass welded unit (PPw)	
Zeolitic nonwelded to partially welded ashflows and bedded, reworked portions of the lower Prow Pass Member and the upper Bullfrog Member of the Crater Flat Tuff.	Upper Crater Flat nonwelded unit (CFUn)	Interval III
Moderately to densely welded, devitrified ashflows of the Bullfrog Member of the Crater Flat Tuff.	Bullfrog welded unit (BFw)	

Table 1 (Concluded)
Description of Units

Description	Reference Stratigraphy Unit Name (Designator)	Zeolitic Zones of Vaniman et al., 1984
Zeolitic partially welded to nonwelded ashflows of the lower Bullfrog Member of the Crater Flat Tuff.	Middle Crater Flat nonwelded unit (CFMn1)	Interval IV
Zeolitic basal bedded, reworked portion of the Bullfrog Member of the Crater Flat Tuff.	Middle Crater Flat nonwelded unit (CFMn2)	Interval IV
Zeolitic, partially welded ashflows of the upper portion of the Tram Member of the Crater Flat Tuff.	Middle Crater Flat nonwelded unit (CFMn3)	Interval IV
Moderately welded, devitrified ashflows of the Tram Member of the Crater Flat Tuff.	Tram welded unit (TRw)	

See Appendix C for listing of former unit designators and correlation with designators established in this report.

Explanation of unit designators

TS w 2

Two or three letter abbreviation of most closely related geologic unit

UO = undifferentiated overburden
TC = Tiva Canyon
PT = Paintbrush (upper)
TS = Topopah Spring
CH = Calico Hills
PP = Prow Pass
CFU = Crater Flat (upper)
BF = Bullfrog
CFM = Crater Flat (middle)
TR = Tram

One letter abbreviation of the general degree of welding

w = welded to moderately welded
n = nonwelded to partially welded

numerical designator of distinctive subunits

Therefore,

* Units TCw, TSw1, TSw2, PPw, BFw, and TRw (Table 1) are not susceptible to zeolitization.

* Units PTn, TSw3, CHn1, CHn2, CHn3, CFUn, CFMn1, CFMn2, and CFMn3 (Table 1) can potentially be zeolitized. Observations at Yucca Mountain indicate that PTn is not extensively zeolitized, whereas all other "n" units are.

In the model, the top of the zone containing prevalent zeolites, TZZ, is a surface of intersection used to divide the reference stratigraphic units into either nonzeolitic zones (above the TZZ surface) or potential zeolitic zones (below the TZZ surface).

Data Input

The analytic technique used by the three-dimensional model requires input data for points of a three-dimensional coordinate system (x,y,z). At Yucca Mountain, the x and y coordinates are defined in Nevada state plane coordinates, whereas the z coordinates are the absolute elevations above mean sea level for the prefaulted units. All coordinates are in feet.

Data were assembled using drill hole locations, lithologic logs, geophysical logs, physical properties, X-ray analyses, and gyroscopic surveys (Appendix B). A drill hole location provides x, y, and z values for the surface position of the hole. The elevation for the base of a given unit (obtained from lithologic logs, geophysical logs, physical property data or X-ray analyses of drill hole samples) is the z value. Drill hole deviations taken from the gyroscopic surveys were used to adjust the three coordinate values (x,y,z).

The x, y, and z coordinates obtained by this procedure are values that represent the locations of surfaces in drill holes. However, some of the points are separated by one or more faults with vertical offset. Before generation of the surfaces, the vertical offset along these faults was removed from the data base (see previous section on Model and Modeling Technique). Removing the offset along a nonvertical fault requires adjustment of each of the coordinate values for data points. A structural block containing drill holes USW G-1, USW G-3, USW GU-3, USW H-3, and USW H-5 was selected as a reference region that was assumed to be unfaulted. All fault offsets were determined relative to this block. Adjustment of coordinates to remove estimated relative fault displacements results in an input data set for generating surfaces that correspond to the prefaulted surfaces.

Vertical displacements of faults were determined in two ways: by using the relative displacements reported by Scott and Bonk (1984) or by adjusting vertical displacements in an iterative procedure to obtain an approximate match between the elevation of predicted and actual outcrop exposures.

The true dips of faults were taken from Scott and Bonk (1984) where available. Otherwise, true fault dips were assumed to be 75 degrees for normal faults and 90 degrees for strike-slip faults based on the average true dips from Scott and Bonk (1984).

Three assumptions were made about the faulting at Yucca Mountain: (1) the assumed offset along known faults does not change with depth along the fault; (2) the dip of the fault does not change at least to the maximum depth of interest; and (3) no faults exist at Yucca Mountain other than those mapped. The input data set as well as the resulting geologic model can be updated easily as new fault information becomes available.

Tables B-1 through B-12 in Appendix B summarize the input data obtained from drill holes. Surface locations and elevations were taken from Holmes and Narver survey information. Drill hole deviations for some depths are from Eastman Whipstock gyroscopic surveys, with deviations at other relevant depths calculated by linear interpolation where necessary. Table B-13 lists the dates on which surveys for each drill hole were made. Table B-14 lists the faults used to adjust the input data, along with the vertical offset and apparent dip estimated for each fault. Figure 4 shows the location of faults, drill holes, and cross sections discussed in this report. The details of the criteria used to define the contacts in each drill hole are described in Appendix B.

Two data points used in the generation of surfaces differ from the corresponding values listed in the tables because of errors during data entry. Input data for the elevation for the Tiva Canyon welded unit (TCw) (Tables 1 and B-5) in USW GU-3 was actually 4514 instead of 4513 and the elevation for the Calico Hills and Lower Paintbrush Tuff nonwelded unit (CHnl) (Tables 1 and B-6) in USW G-4 was 2740 instead of 2743. These minor modifications in the data would not change the resulting predictions significantly, and therefore the analytical surface equations were not recalculated.

In addition to information from the drill holes, two input points (Table B-12) were obtained from surface exposures of the upper, lithophysae-rich subunit of the Topopah Spring welded unit (TSw1). These points were digitized from a preliminary 1:12,000 geologic map of Yucca Mountain (Scott and Bonk, 1984). Both points are in the reference unfaulted block, so correction for fault offsets was not necessary.

The topographic surface used for this model is a digital terrain model which uses a 250 ft grid. The grid points were generated from inclined contours using a weighted average technique. Interpolation between grid points is bilinear. Variations in topography within the 250-ft grid lines are not precisely reproduced.

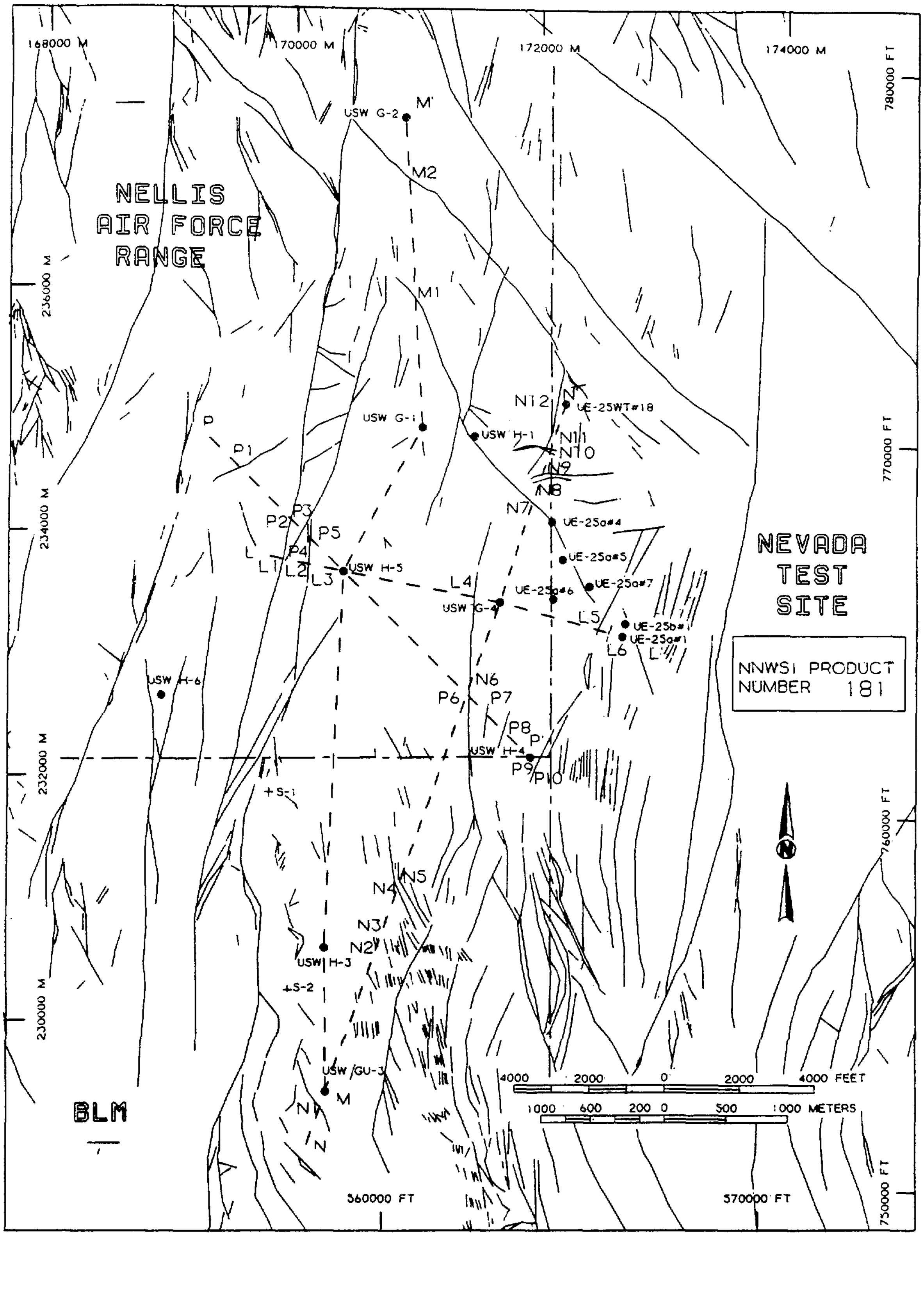

Figure 4. Location of faults, drill holes, and cross sections.

MODEL EVALUATION

The same modeling technique that was used for the three-dimensional model of geologic stratigraphy of Yucca Mountain (Nimick and Williams, 1984) was used to create this reference stratigraphy model. The predictive ability of the technique is discussed by Nimick and Williams (1984, pp. 34-38).

An evaluation of the reliability of the reference stratigraphy model was done by comparing the four cross sections from the model (Figures 5 through 8) to a geologic map, cross sections, and interpretations in Scott and Bonk (1984). Locations of surface outcrops agree within 40 ft (vertical). Thicknesses were consistent.

The boundary of the study area (Figure 1) indicates the area within which the predictive ability of the model has been established. The boundary, in general, corresponds to an outer perimeter defined by drill hole locations. Attempts to extrapolate surfaces outside the study area were not successful. Outside the study area, predicted thicknesses of some of the units increased or decreased dramatically to unreasonable amounts. This results, in part, from the limited number of available input data. In addition, dips vary outside the study area in a manner which the model cannot accommodate at this time.

The elevations of contacts at USW H-6 were predicted before USW H-6 data were included in the model. After allowing for offset on intervening faults, predictions were within about 50 ft of actual elevations. Data from USW H-6 were then added to the model and the surfaces were adjusted to produce the figures in this report.

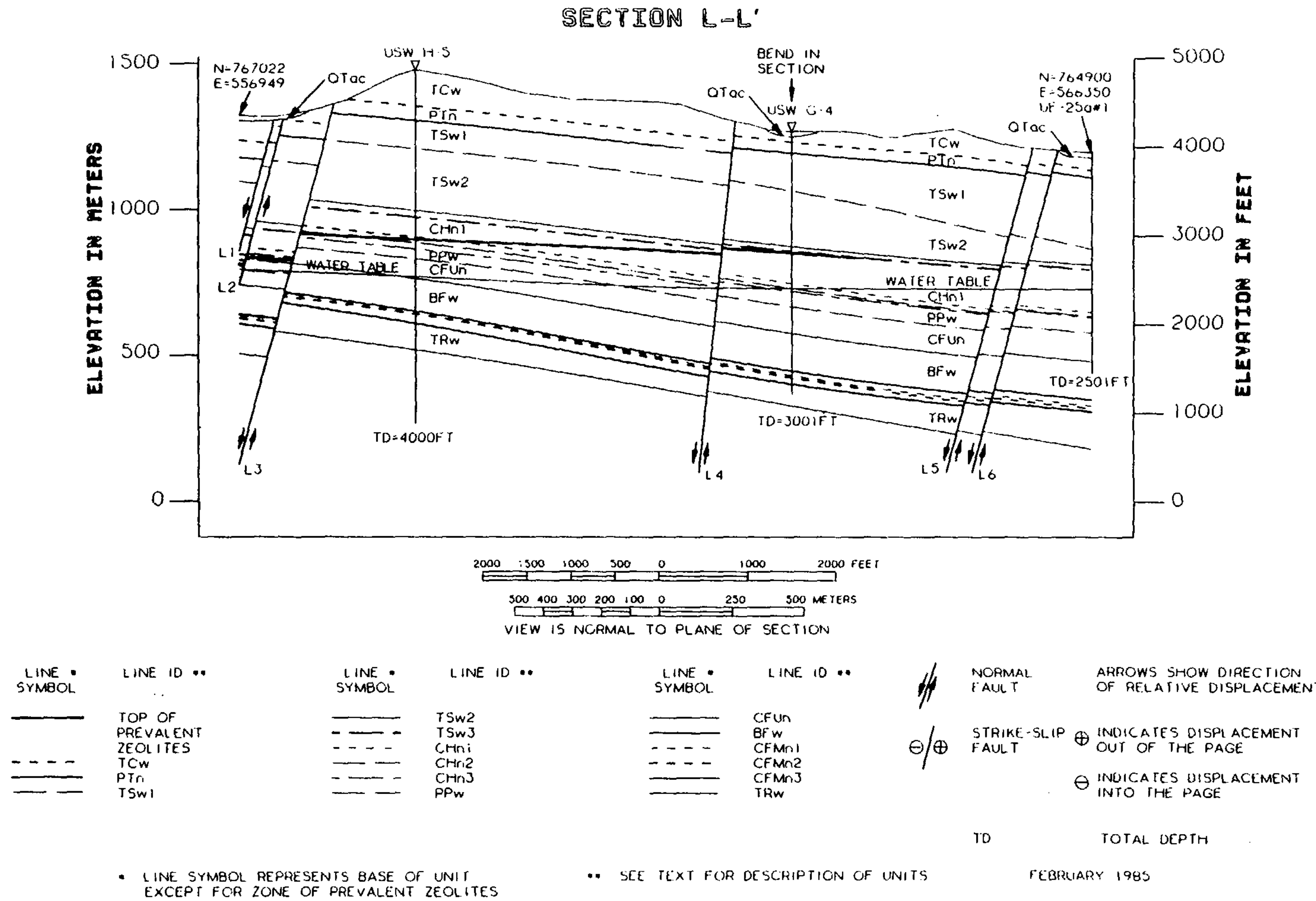

Figure 5. Cross section L-L'. (See Figure 4 for location of cross section and Table 1 for description of unit designators.)

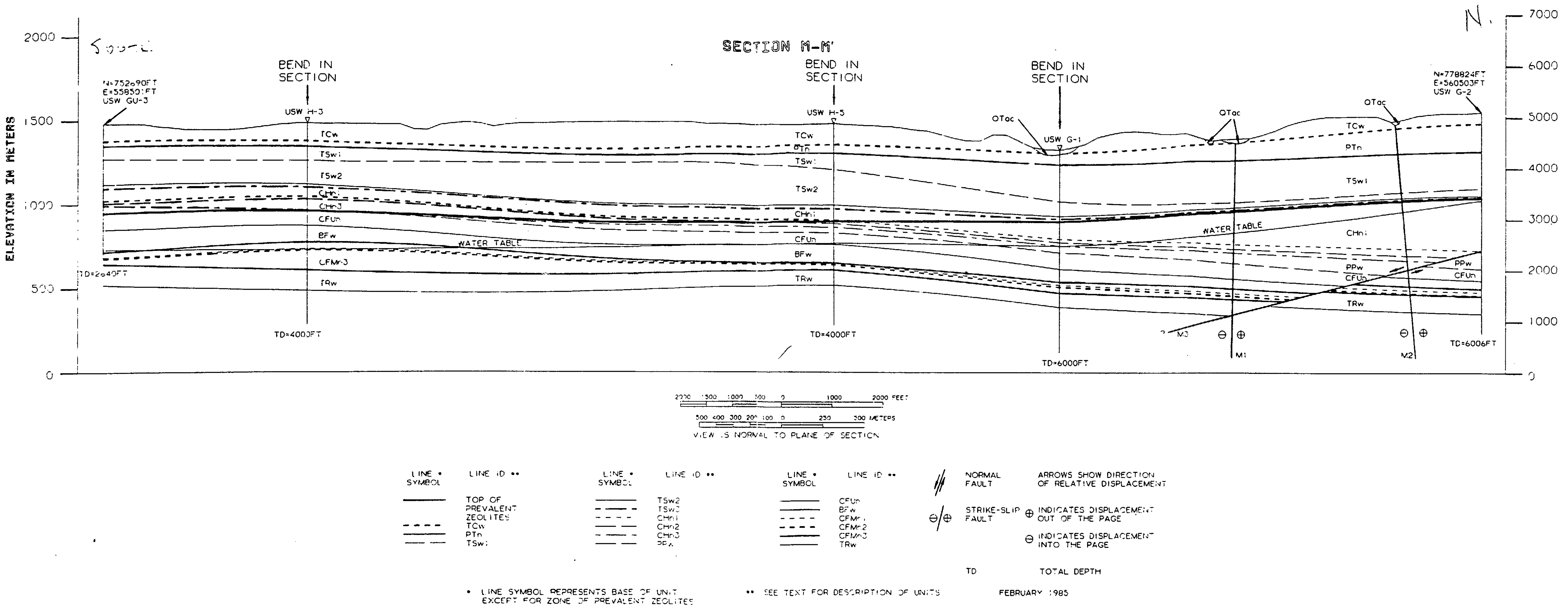

Figure 6. Cross section M-M'. (See Figure 4 for location of cross section and Table 1 for description of unit designators.)

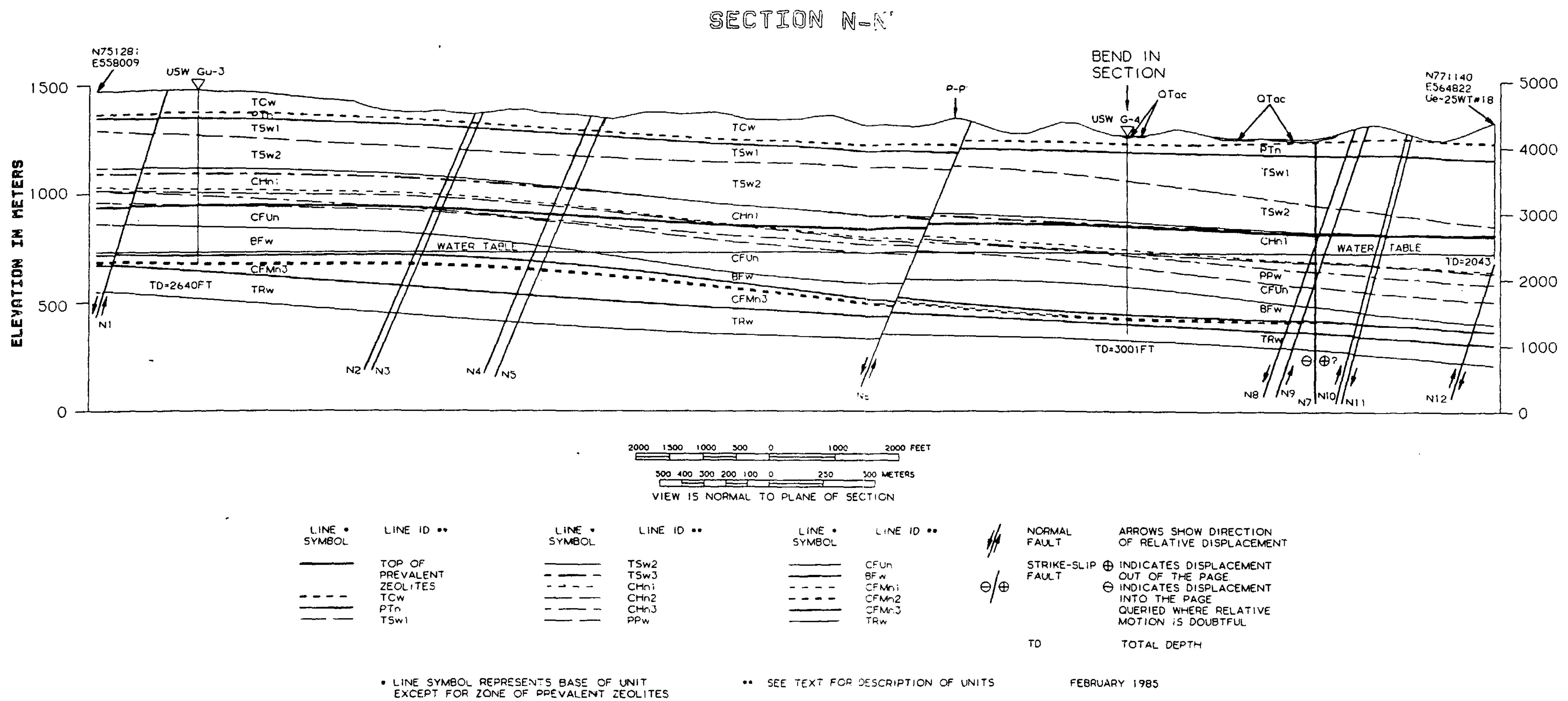

Figure 7. Cross section N-N'. (See Figure 4 for location of cross section and Table 1 for description of unit designators.)

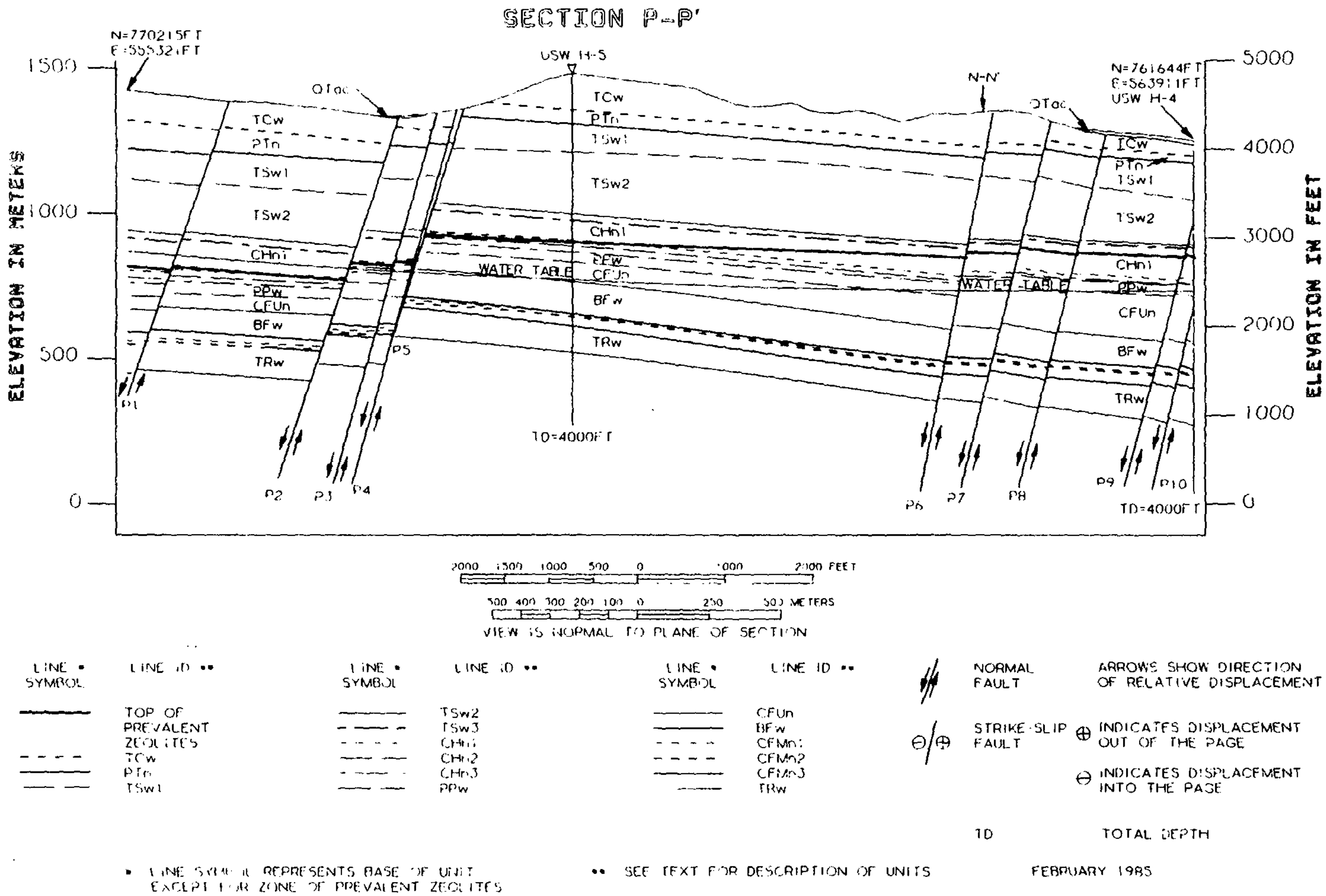

Figure 8. Cross section P-P'. (See Figure 4 for location of cross section and Table 1 for description of unit designators.)

DISCUSSION

The following discussion emphasizes some surfaces important in repository design and performance assessment. First, the thickness of the potential repository host rock, the devitrified, relatively lithophysal-poor, moderately- to densely-welded portion of the Topopah Spring Member of the Paintbrush Tuff (TSw2) will be considered during repository design to determine the placement and orientation of the subsurface repository. The vitrophyre near the base of the Topopah Spring Member (TSw3) is the unit directly beneath the potential repository host rock. The thickness from the repository to the top of the zone of prevalent zeolites (TZZ) is important in influencing radionuclide travel time to the water table and beyond. The distance from the repository to the water table will also influence radionuclide travel time because flow from the subsurface repository to the accessible environment is probably within the unsaturated zone between the repository and the water table (Sinnock et al, 1984, pp. 27-31).

Cross Sections

Four geologic cross sections are shown in Figures 5 through 8. The locations of the cross sections are shown on Figure 4. The cross sections were chosen to intersect drill hole locations, where appropriate, and also to generally cover the study area. The sections show representative information of the three-dimensional model based on the surface-generating algorithms, faults and their corresponding offsets and apparent dips along the section line (Table B-14), location of the water table, and the intersection of the upper surface of the zone containing prevalent zeolites with the reference stratigraphy.

The adjustments to the input data (see Tables B-1 to B-12) resulted in an unfaulted stratigraphy. The fault offsets in Table B-14 were then interactively reinserted in the cross sections in order to bring the elevations of contacts in the drill holes back to their actual positions (Appendix B).

Top of Prevalent Zeolites

The top of the zone containing prevalent zeolites (TZZ) generally corresponds to the top of Interval II of Vaniman et al (1984, pp. 54-56) where Interval II is zeolitized, and to the top of Interval III where Interval II is vitric (for example, in USW GU-3, USW G-3 and USW H-3). Vaniman et al (1984, pp. 54-56) describe Interval II (Table 1) as a relatively thick zone that may occur in the nonwelded and poorly welded tuffs, and in some cases, in the vitrophyre near the base of the Topopah Spring Member of the Paintbrush Tuff and in the tuffaceous beds of Calico Hills. This interval is thin or absent along the crest of Yucca Mountain but thickens down-dip to the east and north. Interval III (Table 1) consists of the poorly welded and bedded tuffs between the Prow Pass and Bullfrog Members of the Crater Flat Tuff. Interval IV consists of the poorly welded and bedded tuffs between the Bullfrog and Tram Members of the Crater Flat Tuff. Interval I of Vaniman et al (1984) occurs at the top of the vitrophyre near the base of the Topopah Spring Member. The interval is typically thin (less than 4 m) and was not included in TZZ. However, Levy (1984, p. 47) notes that if contaminated fluid should escape from the subsurface repository and move downward along fractures, the first strongly sorptive materials (heulandite, smectite, and manganese minerals) encountered would likely be the alteration products within the vitrophyre.

Levy (1984, p. 39) notes that the elevation of zeolitization at Yucca Mountain varies and that the significance of the variation is open to question but may be related to a former position of the regional water table. She also notes that in some areas, the elevation may be controlled more by the original distribution of devitrified and vitric tuff than by the elevation of the water table. Vitric, nonwelded tuffs are much more susceptible to zeolitization than densely welded and devitrified tuffs. She notes (pp. 37-40) that as the transition zone is traced to the south and west of USW G-4, it is located in progressively older units which occur at progressively higher elevations. That trend is also apparent on the cross sections in this report.

The water table presently rises toward the northwestern and northern parts of the study area. The trend of the TZZ surface generally parallels the current water table in unfaulted areas in the central and southeastern portions of the study area. However, the TZZ surface and the water table tend to converge to the north (Figures 6 and 7). If the TZZ surface is related to a former water table, it is reasonable to assume that the water table at the time of zeolitization had a significantly different character, perhaps indicating a difference in topography and recharge areas.

As noted in the previous section, predictions of contacts between the reference units at USW H-6 were checked before adding USW H-6 to the input data. Without the same fault offset as the other units, the predicted elevation of TZZ does not match its actual elevation in the drill hole. The matches are much better using the same fault offsets for TZZ as for the reference stratigraphic units. This suggests that TZZ was probably established before most of the fault displacement took place, although the formation of the TZZ surface and faulting may have been in part concurrent. Levy (1984, pp. 1, 48-49) notes that the last major stage of zeolitization occurred more than 11.3 million years ago, at approximately the same time as the Paintbrush Tuff and older units were being displaced by tilting.

Isopach Maps

Figure 9 is an isopach map of the proposed repository host rock, the lithophysae-poor Topopah Spring welded unit (TSw2). The repository boundary defined by Mansure and Ortiz (1984, pp. 9-20) is included on the figure. The thickness of the proposed repository host rock is 185 ft at UE-25a#1. The unit thickens rapidly toward the west; at USW G-4, it is 621 ft thick. It thins to the north with 290 ft at USW G-1 and 141 ft at USW G-2. The unit does not thin so rapidly to the south. At USW GU-3, it is 497 ft thick. The model indicates a zone of thickening in the west central portion of the area resulting from the rapid change in observed thickness between UE-25a#1 and USW G-4. No input points were available for the interface between the lithophysae-rich Topopah Spring welded unit (TSw1) and the lithophysae-poor Topopah Spring welded unit (TSw2) at USW H-3, USW H-5, and USW H-6. As with any other isopach map or surface map, the predicted contours may change if additional data are added.

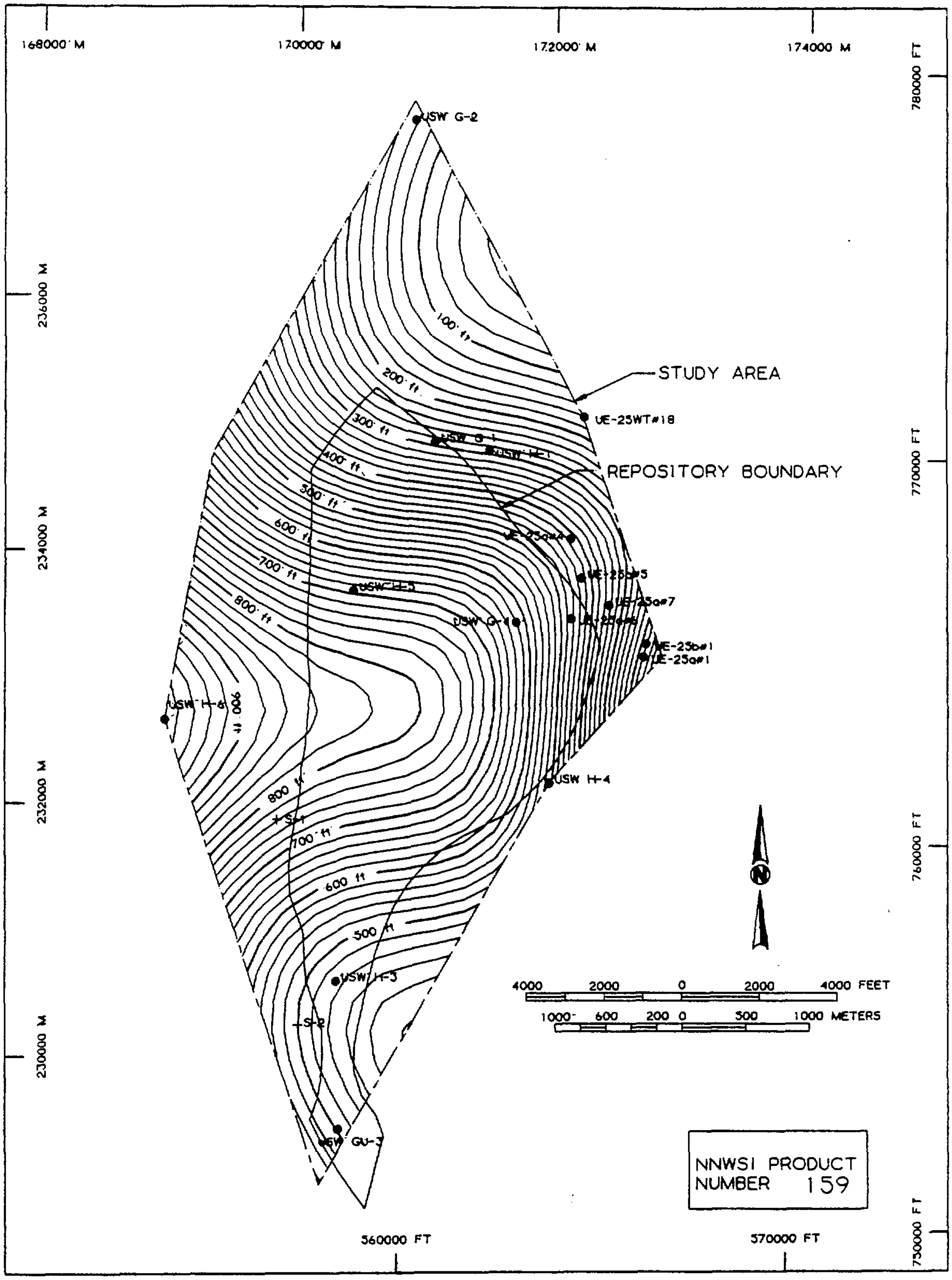

Figure 9. Isopach Map of proposed repository host rock, the devitrified, low-lithophysal moderately to densely welded portion of the Topopah Spring Member of the Paintbrush Tuff (TSw2). Boundary labeled Repository Boundary is tentative boundary proposed by Mansure and Ortiz (1984). Contour interval = 20 ft.

The vitrophyre near the base of the Topopah Spring Member (TSw3) thins gradually from west to east (Figure 10). At USW H-6, the vitrophyre is 90 ft thick while, at UE-25a#1 and USW H-4 the thicknesses are 55 and 32 ft, respectively. The model indicates regions in the eastern portion of the study area where the vitrophyre is absent. The thickness is predicted to be 80 ft at the western edge of the study area. Considering the trend of other units at the site, the thickness of the vitrophyre is probably less variable than indicated.

The distance from the base of the vitrophyre to the TZZ surface (Figure 11) decreases to the northeast from 478 ft at USW GU-3 to only 8 ft at USW G-2, 14 ft at USW G-4, and 0 ft at UE-25a#1. Figures 5 through 8 indicate that the TZZ surface cuts across several units. The nonzeolitized Prow Pass Member is included in the interval between the vitrophyre and the TZZ surface in the southwest portion of the model area (Figure 11) because zeolitization did not extend into the Calico Hills in the southwest portion of the study area. Therefore, some Prow Pass Member is present above the TZZ surface.

The distance between the repository zone defined by Mansure and Ortiz (1984, pp. 9-20) and the water table increases from about 700 ft in the east to over 1400 ft in the southwest (Figure 12). The water table map used in these calculations (Figure 13) is based on information from tabulated groundwater levels in Robison (1984, pp. 6-7). Figure 13 is somewhat modified from a groundwater level map presented in Robison (1984, p. 4) because additional detail was desirable for our calculations.

Uses for the Model

The current model is being used in preliminary hydrologic and radionuclide transport modeling. Finite element meshes can be generated readily either for cross sections or for a single surface based on the ability of the model to generate three-dimensional surfaces throughout the study area. Vertical line

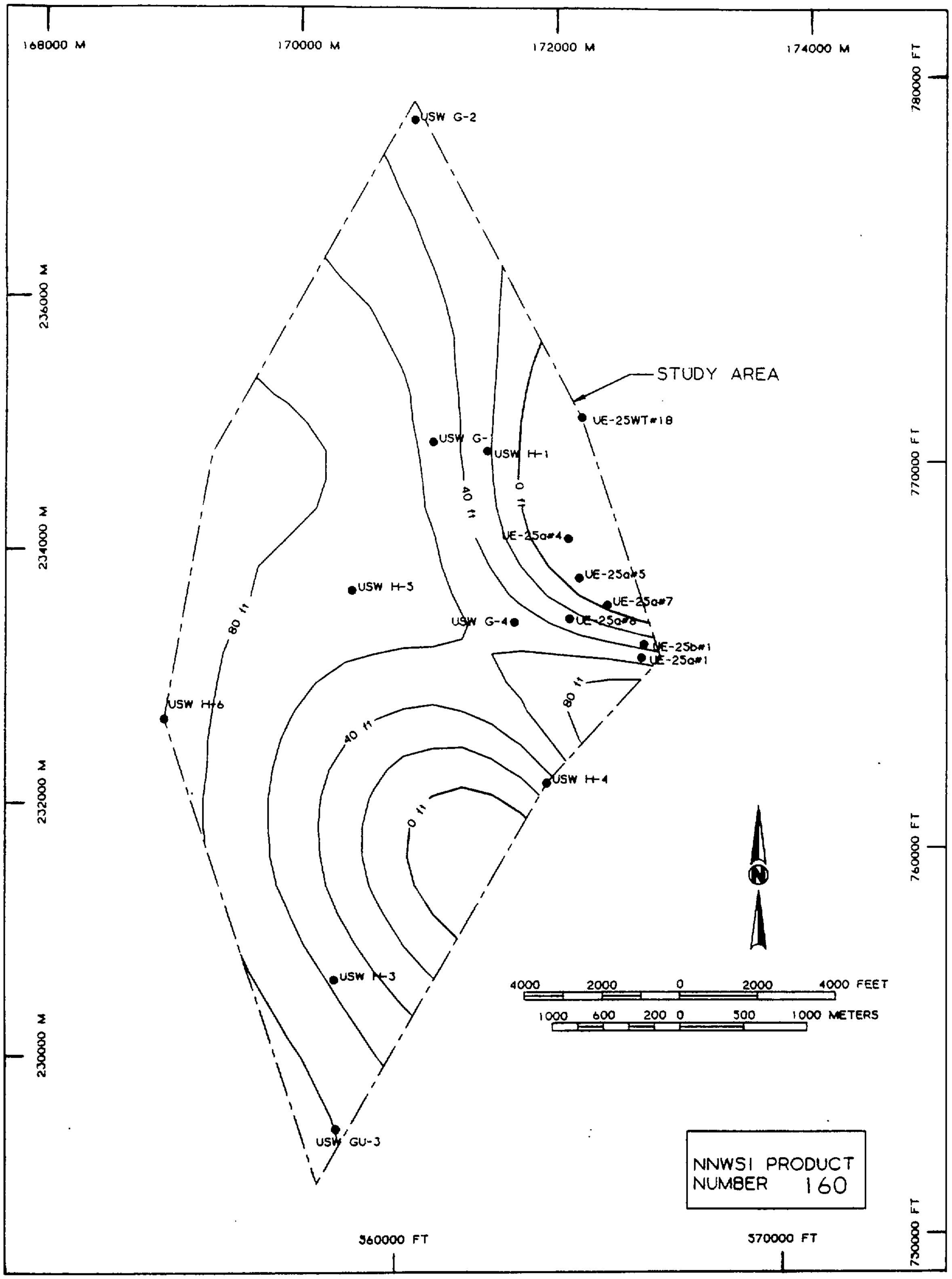

Figure 10. Isopach map of the vitrophyre near the base of the Topopah Spring Member of the Paintbrush Tuff (TSw3). Contour interval = 20 ft.

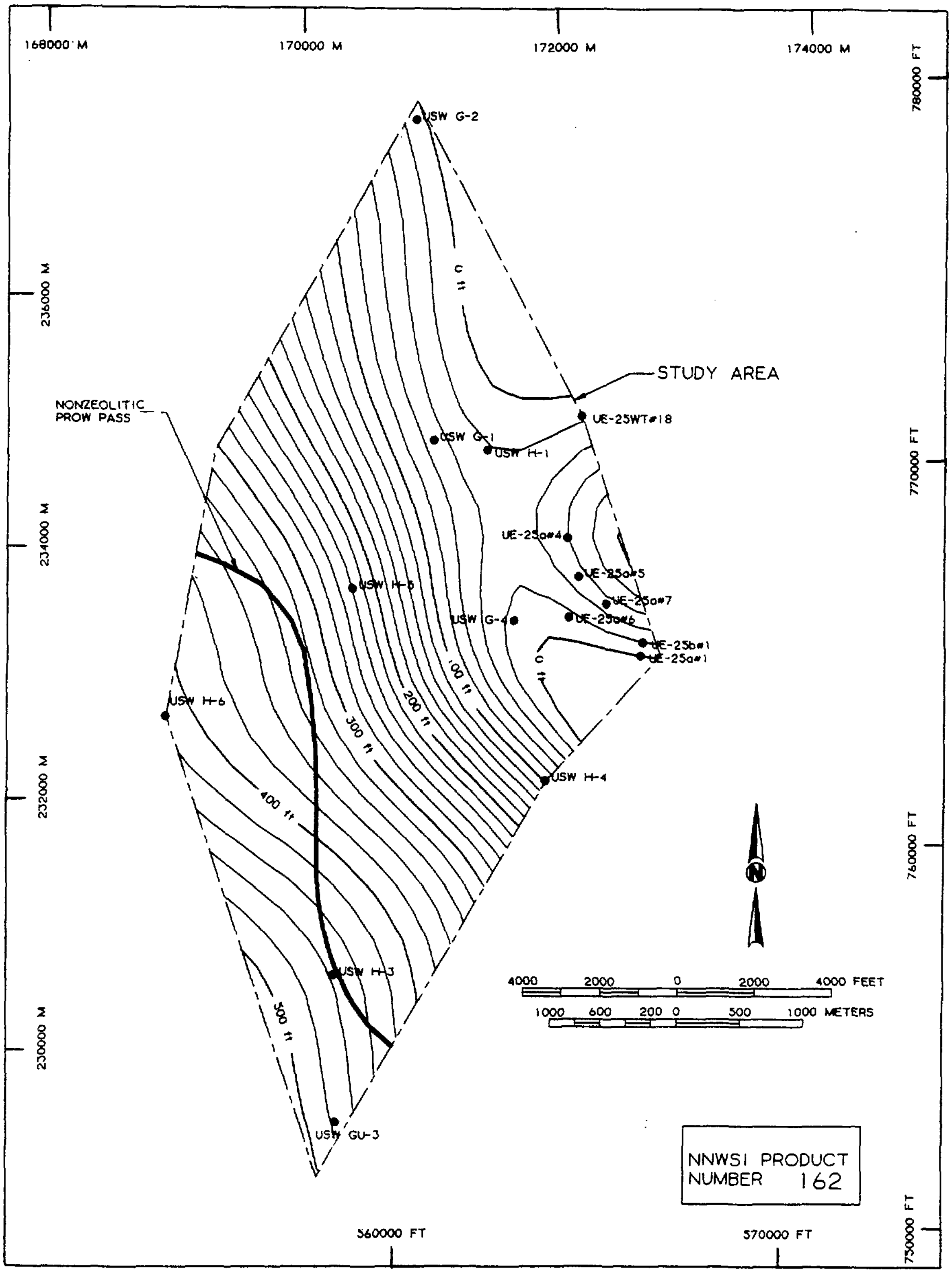

Figure 11. Map of thickness between the vitrophyre near the base of the Topopah Spring Member of the Paintbrush Tuff and the zone of prevalent zeolites. Nonzeolitic Prow Pass (PPw) is included southwest of noted boundary. Contour interval = 20 ft.

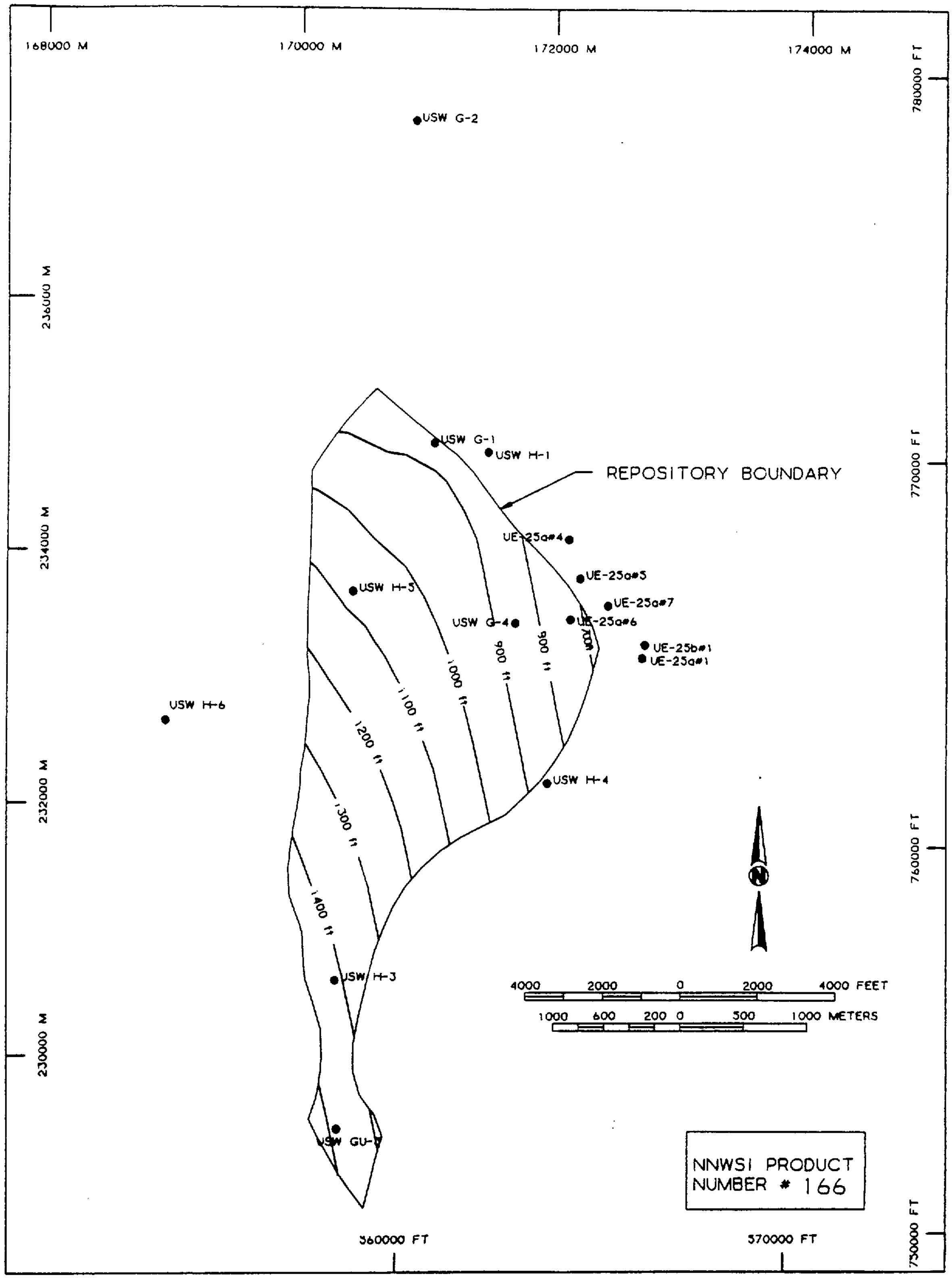

Figure 12. Map of distance between repository horizon [defined in Mansure and Ortiz (1984)] and water table. Contour interval = 100 ft.

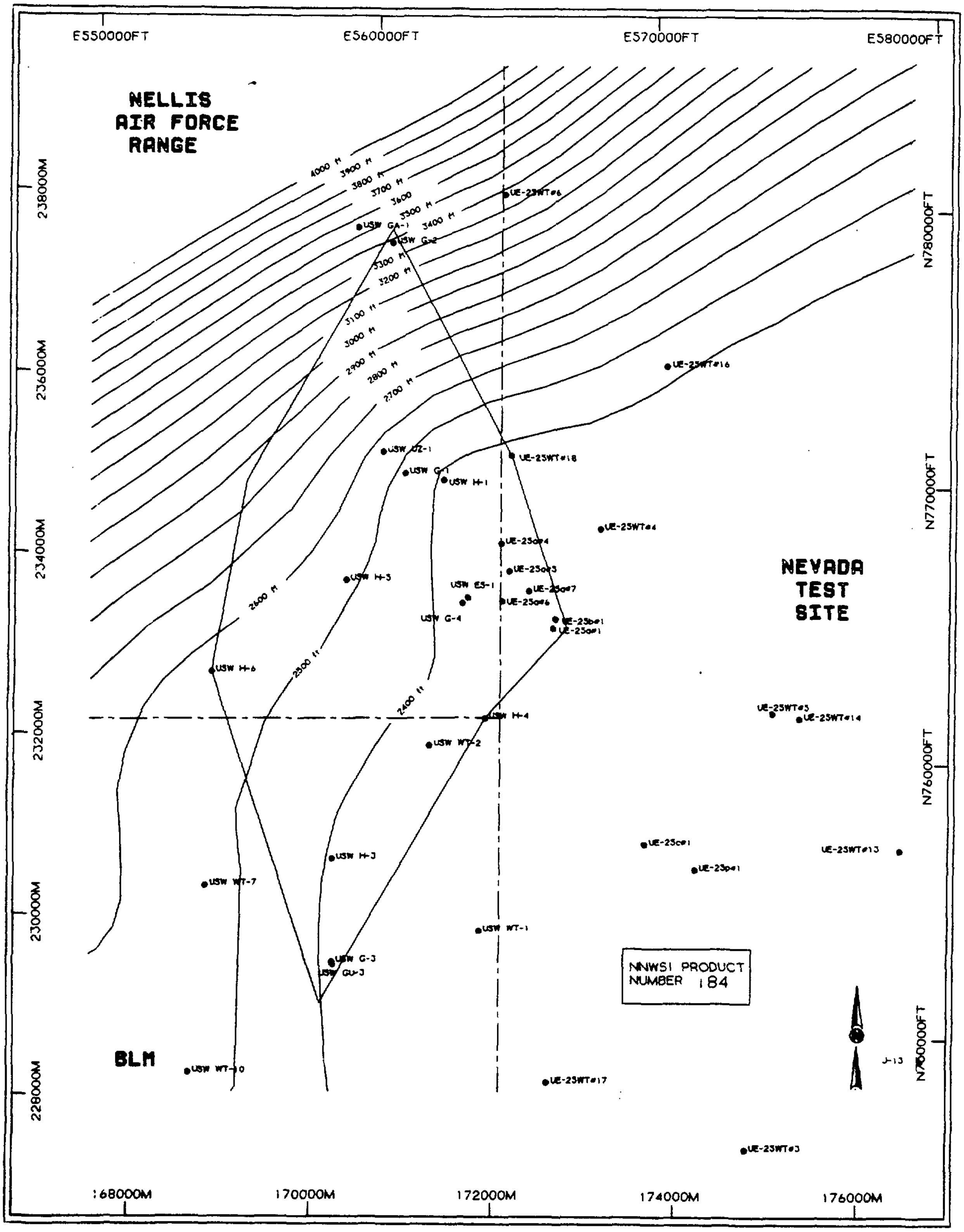

Figure 13. Altitude of the water table above National Geodetic Vertical Datum of 1929. Contour interval = 100 ft.

data can be supplied at any x,y coordinate point, not just at drill holes. The model also has been used to define unit boundaries in a finite element mesh for ongoing in-situ stress calculations. Structure contour and isopach maps can be generated.

The thickness of the proposed repository host rock (TSw2) was used to constrain a preliminary determination of the subsurface area available for a potential repository in that unit (Mansure and Ortiz, 1984). Mansure and Ortiz (1984 p. 6) assumed that a 45-m (148-ft) thick envelope within the proposed repository host rock would be required for the repository. As shown on Figure 9, an adequate thickness of the proposed repository unit exists outside the current, but tentative, repository boundary. Future studies can rely on the model to reassess the best areas for the location of the subsurface repository.

CONCLUSIONS

A three-dimensional model of the reference stratigraphic units at Yucca Mountain is useful in performance assessment and repository design studies involving material properties data because the geometry is reproducible. One-, two-, and three-dimensional data on the geometry of distinct rock units can be obtained for a wide range of applications, including finite element modeling and structure contour map and isopach map development. Development of more detailed three-dimensional models of Yucca Mountain will depend on task-specific requirements. At this time, only one mineralogical surface is included in the model. However, in the future, a mineralogical and geochemical stratigraphy will be developed and modeled. For example, it is possible to model the distribution of individual parameters such as hydraulic conductivity, sorption potential, porosity, thermal conductivity, or mechanical properties if enough data exist to justify a three-dimensional representation.

As with the geologic model of Yucca Mountain (Nimick and Williams, 1984), a major shortcoming of the reference stratigraphic model at this time is the absence of a comprehensive three-dimensional description of the area-wide fault system. The current fault descriptions lack the detail sufficient to automate the removal of fault movement from input data or its reinsertion into calculated surfaces. Therefore, faulting effects are handled interactively. However, the model is evolving, and in the future, an attempt will be made to improve the modeling treatment of faults. In addition, the model may be improved by the addition of the dip of beds as an input parameter and the addition of a statistical uncertainty measure. The three-dimensional model will also be improved at intervals as additional data from outcrops or from new drill holes become available.

REFERENCES

Applicon Inc., AGS/880 Users Guide, M-4080, 32 Second Avenue, MA 01803.

Bentley, C. B., Robison, J. H., and Spengler, R. W., 1983, "Geohydrologic Data for Test Well USW H-5, Yucca Mountain Area, Nye County, Nevada"; US Geological Survey Open-File Report 83-853.

Bish, D., 1984, Personal communication, 1/30/84.

Caporuscio, F., Vaniman, D., Bish, D., Broxton, D., Arney, B., Heiken, G., Byers, F., Gooley, R., and Semarge, E., 1982, "Petrologic Studies of Drill Cores USW-G2 and UE25b-1H, Yucca Mountain, Nevada"; Los Alamos National Laboratory Report LA-9255-MS.

Carroll, P. I., Caporuscio, F. A., and Bish, D. L., 1981, "Further Description of the Petrology of the Topopah Spring Member of the Paintbrush Tuff in Drill Holes UE25A-1 and USW-G1 and of the Lithic-Rich Tuff in USW-G1, Yucca Mountain, Nevada"; Los Alamos National Laboratory Report LA-9000-MS.

Craig, R. W., Reed, R. L., and Spengler, R. W., 1983, "Geohydrologic Data for Test Well USW H-6, Yucca Mountain Area, Nye County, Nevada"; US Geological Survey Open-File Report 83-856.

Lappin, A. R., Van Buskirk, R. G., Enniss, D. O., Butters, S. W., Prater, F. M., Muller, C. S., and Bergosh, J. L., 1982, "Thermal Conductivity, Bulk Properties, and Thermal Stratigraphy of Silicic Tuffs from the Upper Portion of Hole USW-G1, Yucca Mountain, Nye County, Nevada"; Sandia National Laboratories Report SAND81-1873.

Levy, S. S., 1984, Petrology of Samples from Drill Holes USW H-3, H-4, and H-5, Yucca Mountain Nevada"; Los Alamos National Laboratory Report LA-9706-MS.

Lobmeyer, D. H., Whitfield, M. S.,Jr., Lahoud, R. G., and Bruckheimer, L., 1983, "Geohydrologic Data for Test Well UE-25b#1, Nevada Test Site, Nye County, Nevada"; US Geological Survey Open-File Report 83-855.

Maldonado, F. and Koethers, S. L., 1983, "Stratigraphy, Structure, and Some Petrographic Features of Tertiary Volcanic Rocks at the USW G-2 Drill Hole, Yucca Mountain, Nye County, Nevada"; US Geological Survey Open-File Report 83-732.

Mansure, A. J., and Ortiz, T. S., 1984, "Preliminary Evaluation of the Subsurface Area Available for a Potential Nuclear Waste Repository at Yucca Mountain"; Sandia National Laboratories Report SAND84-0175.

Nimick, F. B. and Williams, R. L., 1984, "A Three-Dimensional Geologic Model of Yucca Mountain, Southern Nevada"; Sandia National Laboratories Report SAND83-2593.

Nimick, F. B., Bauer, S. J., and Tillerson, J. R., 1984, "Recommended Matrix and Rock-Mass Bulk, Mechanical and Thermal Properties for Thermomechanical Stratigraphy of Yucca Mountain, Version I"; Sandia National Laboratories, Keystone Document 6310-85-1.

Robison, J. H., 1984, "Ground-water Level Data and Preliminary Potentiometric-surface Maps, Yucca Mountain and Vicinity, Nye County, Nevada"; U.S. Geological Survey Water-Resources Investigations Report 84-4197.

Rush, F. E., Thordarson, W., and Bruckheimer, L., 1983, "Geohydrologic and Drill-Hole Data for Test Well USW H-1, Adjacent to Nevada Test Site, Nye County, Nevada"; US Geological Survey Open-File Report 83-141.

Schwartz, B.M., 1983, "Bulk Properties of Core Samples from Hole USWGU3"; Sandia National Laboratories Memo to A.R.Lappin, 1/13/83.

Scott, R. B., R. W. Spengler, S. Diehl, A. R. Lappin, and M. P. Chornack, 1983, "Geologic Character of Tuffs in the Unsaturated Zone at Yucca Mountain, Southern Nevada", in Role of the Unsaturated Zone in Radioactive and Hazardous Waste Disposal, edited by J. Mercer, R. Rao, and I. Marine, Ann Arbor Science, Ann Arbor, Michigan, p. 289-335.

Scott, R. B. and Castellanos, M., 1984, "Stratigraphic and Structural Relations of Volcanic Rocks in Drill Holes USW GU-3 and USW G-3, Yucca Mountain, Nye County, Nevada"; US Geological Survey Open-File Report 84-491.

Scott, R. B. and Bonk, J., 1984, "Preliminary Geologic Map of Yucca Mountain, Nye County, Nevada with Geologic Sections"; US Geological Survey Open-File Report 84-494.

Sinnock, S., Lin, Y. T., and Brannen, J. P., 1984, "Preliminary Bounds on the Expected Postclosure Performance of the Yucca Mountain Repository Site, Southern Nevada"; Sandia National Laboratories Report SAND84-1492.

Spengler, R. W., Byers, F. M.,Jr., and Warner, J. B., 1981, "Stratigraphy and Structure of Volcanic Rocks in Drill Hole USW-G1, Yucca Mountain, Nye County, Nevada"; US Geological Survey Open-File Report 81-1349.

Spengler, R. W. and Chornack, M. P., 1984, "Stratigraphic and Structural Characteristics of Volcanic Rocks in Core Hole USW G-4, Yucca Mountain, Nye County, Nevada" with a section on geophysical logs by D. C. Muller and J. Kibler; US Geological Survey Open-File Report 84-789.

Spengler, R. W., Muller, D. C., and Livermore, R. B., 1979, "Preliminary Report on the Geology and Geophysics of Drill Hole UE25a-1, Yucca Mountain, Nevada"; US Geological Survey Open-File Report 79-1244.

Spengler, R. W. and Rosenbaum, J. G., 1980, "Preliminary Interpretations of Geologic Results Obtained from Boreholes UE25a-4, -5, -6, and -7, Yucca Mountain, Nevada Test Site"; US Geological Survey Open-File Report 80-929.

Sykes, M. L., Heiken, G. H., and Smyth, J. R., 1979, "Mineralogy and Petrology of Tuff Units from the UE25a-1 Drill Site, Yucca Mountain, Nevada"; Los Alamos National Laboratory Report LA-8139-MS.

Thordarson, W., Rush, F. E., Spengler, R. W., and Waddell, S. J., 1984, "Geohydrologic and Drill-Hole Data for Test Well USW H-3, Yucca Mountain, Nye County, Nevada"; US Geological Survey Open-File Report 84-149.

Vaniman, D., Bish, D., Broxton, D., Byers, F., Heiken, G., Carlos, B., Semarge, E., Caporuscio, F., and Gooley, R., 1984, "Variations in Authigenic Mineralogy and Sorptive Zeolite Abundance at Yucca Mountain, Nevada, Based on Studies of Drill Cores USW GU-3 and G-3"; Los Alamos National Laboratory Report LA-9707-MS.

Waters, A. C. and Carroll, P. R. (eds.), 1981, "Preliminary Stratigraphic and Petrologic Characterization of Core Samples from USW-G1, Yucca Mountain, Nevada"; Los Alamos National Laboratory Report LA-8840-MS.

Whitfield, M. S., Jr., Thordarson, W., and Eshom, E. P., 1984, "Geohydrologic and Drill-Hole Data for Test Well USW H-4, Yucca Mountain, Nye County, Nevada"; US Geological Survey Open-File Report 84-449.

Williams, R. L. and Nimick, F. B., in preparation, "Technique for the Geometric Modeling of Underground Surfaces"; Sandia National Laboratories Report SAND84-0307.

APPENDIX A

GRAPHICS PROCEDURES

The procedures described in this appendix are implemented on the Applicon 885 Graphics System. For a more detailed description of the system, see the Applicon Inc. AGS/880 users guide.

A nongraphic data file must exist, containing a collection of surface definition equations--one definition for each surface to be displayed or interacted with by the graphics system. Each definition (a set of coefficients) is identified in the file by a unique name identifier.

Procedures used in Cross Section Development

Define the Line of Section - The line of section is entered into the graphics data base either by keyboard entry of given endpoints or from digitized points.

Define the Resolution - The smoothness of the curvature in the units to be displayed in the cross section is determined by the number and position of the intermediate points in the line of section. In the cross sections for this report, points were inserted at a spacing of from 200 to 250 ft. Additional points can be added at any time to enhance the resolution.

Define Surface-Line Association - A copy of the section line is made for each surface to appear in the section. Each line is given the unique graphics name that correlates with one of the surface definitions in the nongraphics data file.

Project Line of Section to Surface - The lines are vertically projected to their respective surface locations by calculation of a new z coordinate using an AGS user command developed at SNLA.

Pinch Out of Displayed Units - Lines crossing other lines indicate that a unit has been pinched out. The appropriate line segments are hidden where the corresponding unit is absent. This procedure may vary between the different types of sections and units being displayed.

Add Faults - Any faults that intersect the cross section line are initiated at the intersection with the ground surface line and are rotated into the line of section at the given dip (see Table B-14).

Offset Faulted Surfaces - Lines intersecting a fault are offset by the values given for each fault (see Table B-14). This offset adjustment is made for all units simultaneously. The adjustment is made in elevation only.

Plot Output - When the above operations have been completed, a copy of the cross section is rotated into an orthogonal view and is labeled as required. The finished plot is then output at the desired scale.

Procedures Used in Surface Contour Map Development

Generate the Mesh - A mesh is constructed at the required resolution using lines with vertices at grid line intersections. The mesh is copied and named to select the surface desired. For the maps in this report, the grid resolution is 750 ft.

Project the Mesh - The AGS user command projects the mesh to the corresponding surface in the specified data file.

Contour the Mesh - Given the required contour interval, the system is placed into Section Mode and lines are added between the points that are the intersection of the mesh and a horizontal plane positioned at the desired elevation. This is performed interactively for each elevation to be contoured.

Plot Output - When the above operations have been completed, the map is labeled as required and the plot is output at the desired scale.

Procedures Used in Isopach Map Development

Generate the Mesh - A mesh is constructed at the required resolution as for surface contour maps and named according to the base of the unit to be contoured.

Project the Mesh - An AGS user command projects the mesh to the corresponding surface in the specified data file.

Generate Thickness Mesh - An isopach map is represented by a mesh that has z coordinate (elevation) values that correspond to the difference in elevations between two surfaces. The previously projected mesh is renamed to the top of the unit to be contoured. Another AGS user command developed at SNLA modifies the z coordinates of the mesh to that of the calculated difference between the two surfaces.

Contour the Thickness Mesh - Given the required contour interval, the system is placed into Section Mode and lines are added between the points that are the intersection of the thickness mesh and a horizontal plane position at the desired thickness value.

Plot Output - When the above operations have been completed, the map is labeled as required and the plot is output at the desired scale.

APPENDIX B

CRITERIA FOR CONTACT DEFINITION AND LOCATION

This appendix describes the information used to assign depths for the contacts of reference stratigraphy units in the drill holes at Yucca Mountain. Figure B-1 is a correlation between the reference stratigraphy and the geologic stratigraphy.

In addition, Tables B-1 through B-12 list the data from the drill holes that were used to generate the reference thermal/mechanical and hydrological stratigraphic model. Table B-13 lists the dates on which gyroscopic surveys for each drill hole were made. Table B-14 lists the faults used to adjust the input data, along with the vertical offset and apparent dip estimated for each fault.

An uncertainty described by a "+" symbol indicates that the contact could be at a greater depth, while a "-" indicates the possibility of a shallower depth.

Information Sources for Contacts between Reference Stratigraphic Units

UE-25a#1

TCw	Transition from devitrified to vitric tuff in lithologic log.
PTn	Transition from devitrified to vitric tuff in lithologic log, adjusted with information from Carroll et al (1981, pp. 10, 16) as described in Nimick and Williams (1984, p. 18).
TSw	Contact taken to be the base of the lowermost ashflow in the Topopah Spring Member containing 10-20% lithophysae, as described in the lithologic log.
TSw2	Transition from devitrified tuff to vitrophyre in lithologic log.
TSw3	Transition from vitrophyre to vitric ashflow in lithologic log.
CHn1	Transition from ashflow to basal bedded unit of the Tuffaceous Beds of the Calico Hills in lithologic log.
CHn2	Transition from bedded unit to ashflow in lithologic log.
CHn3	The uppermost ashflow in the Prow Pass Member is non- to partially welded (lithologic log) and is assumed to be zeolitized. Sykes et al (1979, p. 65) describe a devitrified sample from the underlying ashflow. Contact assigned at the boundary between the two ashflows. Uncertainty: +7 ft.
PPw	Data indicate a sharp increase in porosity between samples at depths of 1999.6 and 2025.7 ft. Contact assigned at midpoint of the interval. Uncertainty: +13 ft, -13 ft.

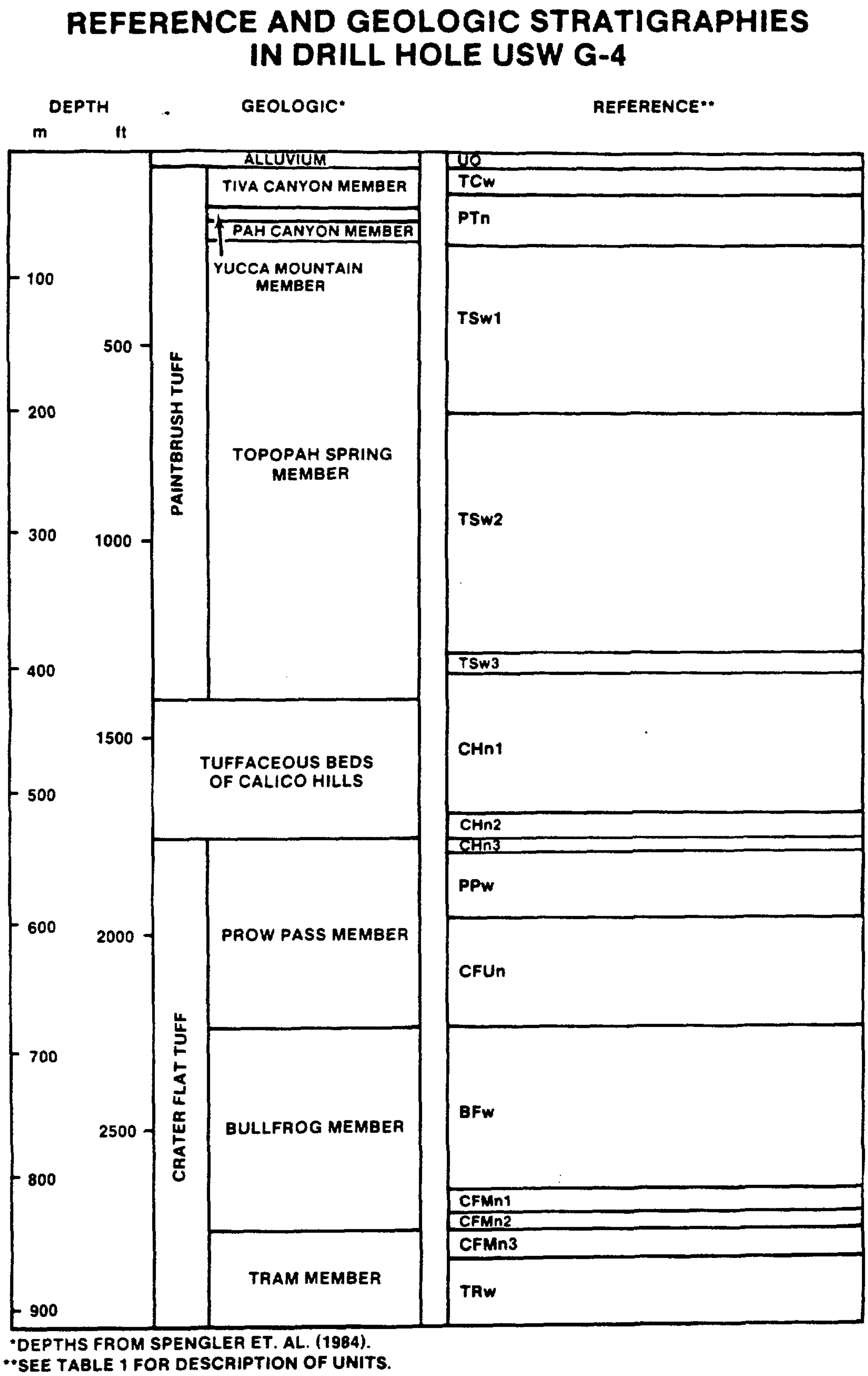

Figure B-1. Correlation between the Reference Stratigraphy and the Geologic Stratigraphy.

CFUn Data indicate a sharp increase in grain density between depths of 2331.4 and 2341.0 ft. Contact assigned at midpoint of interval. Uncertainty: +5 ft, -5 ft.

TZZ Sykes et al (1979, p. 55) state that a sample at a depth of 1324 ft is altered to clinoptilolite. This is 7 ft below the base of Unit TSw3, so all of Unit CHn1 is assumed to be zeolitized. Contact assigned at base of Unit TSw3. Uncertainty: +7 ft.

Sources of information:

Lithologic Log: Spengler et al (1979, pp. 12-20)
Mineralogy: Sykes et al (1979, pp. 31-76), Carroll et al (1981, p. 10)

UE-25a#4

TCw Transition from devitrified to vitric tuff in lithologic log.

PTn Transition from vitric tuff to devitrified tuff in lithologic log.

Sources of information:

Lithologic Log: Spengler and Rosenbaum (1980, pp. 10-11)

UE-25a#5

TCw Transition from devitrified to vitric tuff in lithologic log.

PTn Transition from vitric tuff to devitrified tuff in lithologic log.

Sources of information:

Lithologic log: Spengler and Rosenbaum (1980, pp. 12-13)

UE-25a#6

TCw Transition from devitrified to vitric tuff in lithologic log.

Ptn Transition from vitric tuff to devitrified tuff in lithologic log.

Sources of information:

Lithologic log: Spengler and Rosenbaum (1980, pp. 14-15)

UE25a#7

TCw Transition from devitrified to vitric tuff in lithologic log.

PTn Transition from vitric tuff to devitrified tuff in lithologic log.

Sources of information:

Lithologic log: Spengler and Rosenbaum (1980, pp. 16-18)

UE-25b#1

PTn Transition from devitrified to vitric tuff in lithologic log.

TSw1 Transition from vitric tuff to devitrified tuff in lithologic log.

TSw2 Transition from devitrified tuff to vitrophyre in lithologic log.

TSw3 Transition from vitrophyre to vitric ashflow in lithologic log.

CHn1 Transition from ashflow to basal bedded unit of the Tuffaceous Beds of the Calico Hills in lithologic log.

CHn2 Transition from bedded unit to ashflow in lithologic log.

CHn3 Contact assigned at bottom of the uppermost ashflow of the Prow Pass Member based on mineralogy descriptions in the lithologic log.

PPw Data indicate a sharp decrease in grain density at depths between 2071 and 2101 ft. Contact assigned at midpoint of this interval. Uncertainty: +15 ft, -15 ft.

CFUn Data show low grain density at 2390.1 ft, high grain density at 2411.9 ft. X-ray data indicate sample at 2402 ft is devitrified. Contact assigned midway between low grain density depth and devitrified depth. Uncertainty: +6 ft, -6 ft.

BFw Data indicate a sharp decrease in grain density at depths between 2783.85 and 2790.7 ft. Contact assigned at midpoint of interval. Uncertainty: +3 ft, -3 ft.

CFMn1 Transition from ashflow to bedded tuff in lithologic log.

CFMn2 Transition from bedded tuff to ashflow in lithologic log.

CFMn3 Data indicate an increase in grain density at depths between 2919.6 and 2924.7 ft. Contact assigned at midpoint of interval. Uncertainty: +3 ft, -3 ft.

TRw Data show an increase in porosity at depths between 3323.0 and 3340.1 ft. X-ray data show trace zeolitization at 3298 ft and slight zeolitization at 3326 and 3362 ft. Contact assigned midway between low porosity sample depth and 3326 ft. Uncertainty: +2 ft, -2 ft.

TZZ Contact assigned at the base of the lowermost ashflow of the Topopah Spring Member based on mineralogic descriptions in the lithologic log.

Sources of information:

Lithologic log: Lobmeyer et al (1983, pp. 7-16)
Mineralogy: Caporuscio et al (1982, pp. 14-15)

USW G-1

PTn Transition from vitric tuff to devitrified tuff in lithologic log.

TSw1 Contact assigned at the base of the lowermost ashflow in the Topopah Spring Member containing 10-20% lithophysae as described in the lithologic log.

TSw2 Transition from devitrified tuff to vitrophyre in lithologic log.

TSw3 Transition from vitrophyre to vitric ashflow in lithologic log.

CHn1 Transition from ashflow to basal bedded unit of Tuffaceous Beds of Calico Hills in lithologic log.

CHn2 Transition from bedded unit to ashflow in lithologic log.

CHn3 X-ray data indicate the presence of extensive zeolitization at a depth of 1854 ft and a mineral assemblage indicative of devitrification at 1883 ft. Contact assigned at the midpoint of the interval. Uncertainty: +15 ft, -15 ft.

PPw Data indicate a decrease in grain density at depths between 1984.7 and 2010 ft. Contact assigned at the midpoint of the interval. Uncertainty: +13 ft, -13 ft.

CFUn — X-ray data indicate the presence of extensive zeolitization at a depth of 2316 ft and a mineral assemblage indicative of devitrification at 2318 ft. Contact assigned at the midpoint of the interval. Uncertainty: +1 ft, -1 ft.

BFw — Data indicate a decrease in grain density at depths between 2538 and 2549 ft. Contact assigned at the midpoint of the interval. Uncertainty: +6 ft, -6 ft.

CFMn1 — Transition from ashflow to bedded tuff in lithologic log.

CFMn2 — Transition from bedded tuff to ashflow in lithologic log.

CFMn3 — Data indicate an increase in grain density at depths between 2748 and 2761 ft. Contact assigned at the midpoint of the interval. Uncertainty: +7 ft, -7 ft.

TRw — X-ray data indicate the presence of a mineral assemblage indicative of devitrification at a depth of 3001 ft and extensive zeolitization at 3053 ft. Contact assigned at the midpoint of the interval. Uncertainty: +26 ft, -26 ft.

TZZ — Data indicate an increase in grain density at depths between 1385.2 and 1394.9 ft. X-ray data show that glass is the dominant phase at a depth of 1357 ft and slight zeolitization at 1392 ft. Contact assigned midway between 1392 and 1394.9 ft. Uncertainty: +1 ft, -1 ft.

Sources of information:

Lithologic log: Spengler et al (1981, pp. 11-25)
Mineralogy: Waters and Carroll (1981, pp. 62-66)

USW G-2

TCw — Transition from devitrified to vitric tuff in lithologic log.

PTn — Transition from vitric tuff to devitrified tuff lithologic log.

TSw1 — Contact assigned at the base of the lowermost ashflow in the Topopah Spring Member containing 10-20% lithophysae, based on the lithologic log.

TSw2 — Transition from devitrified tuff to vitrophyre in lithologic log.

TSw3	Transition from vitrophyre to vitric ashflow tuff in lithologic log.
CHn1	Lower contact in drill hole is a fault, as described in the lithologic log. Contact is assumed to be colocated with the fault.
CHn2	Absent due to faulting. Original thickness assumed to be 146 ft.
CHn3	X-ray data indicate extensive zeolitization at a depth of 2667 ft and a mineral assemblage indicative of devitrification at 2744 ft. Bulk property data show low grain densities through a depth of 2699.9 ft. Contact assigned at a depth of 2703 ft based on the density log. Uncertainty: +41 ft, -3 ft.
PPw	X-ray data show a mineral assemblage indicative of devitrification at a depth of 3037 ft and extensive zeolitization at 3067 ft. Contact assigned at the midpoint of the interval. Uncertainty: +15 ft, -15 ft.
CFUn	X-ray data indicate extensive zeolitization at a depth of 3250 ft and a mineral assemblage indicative of devitrification at 3308 ft. Bulk property data indicate an increase in grain density at depths between 3243 and 3305 ft. Contact assigned midway between 3250 and 3305 ft. Uncertainty: +28 ft, -28 ft.
BFw	Data indicate a decrease in grain density at depths between 3433.2 and 3439.2 ft. Contact assigned at a depth of 3439 ft, based on the epithermal neutron porosity log. Uncertainty: +0 ft, -6 ft.
CFMn1	Transition from ashflow to bedded tuff in lithologic log.
CFMn2	Transition from bedded tuff to ashflow in log.
CFMn3	X-ray data indicate extensive zeolitization at a depth of 3578 ft and a mineral assemblage indicative of devitrification at 3627 ft. Bulk property data show an increase in grain density at depths between 3563.2 and 3600 ft. Contact assigned at a depth of 3579 ft, based on the epithermal neutron porosity log. Uncertainty: +21 ft, -1 ft.
TRw	X-ray data show a mineral assemblage indicative of devitrification at a depth of 3908 ft and extensive zeolitization at 3933 ft. Bulk property data indicate a decrease in grain density at depths between 3894.8 and 3914.0 ft. Contact assigned midway between 3908 and 3914 ft. Uncertainty: +3 ft, -3 ft.

TZZ X-ray data indicate show that glass is the dominant phase at a depth of 1664 ft and extensive zeolitization occurs at 1691 ft. Contact assigned at the midpoint of the interval. Uncertainty: +14 ft, -14 ft.

Sources of information:

Lithologic log: Maldonado and Koether (1983, pp. 56-83)
Mineralogy: Caporuscio et al (1982, pp. 11-13)

USW GU-3

TCw Transition from devitrified to vitric tuff in lithologic log.

PTn Transition from vitric to devitrified tuff in lithologic log.

TSw1 Contact assigned at the base of the lowermost ashflow of the Topopah Spring Member, which contains 10-20% lithophysae, based on the description in the lithologic log.

TSw2 Transition from devitrified tuff to vitrophyre lithologic log.

TSw3 Transition from vitrophyre to vitric ashflow in lithologic log.

CHn1 Transition from ashflow to basal bedded unit of the Tuffaceous Beds of the Calico Hills in lithologic log.

CHn2 Transition from bedded unit to ashflow in lithologic log.

CHn3 X-ray data indicate a change from glass to a mineral assemblage indicative of devitrification at depths between 1598.5 and 1603 ft. Contact assigned at the midpoint of the interval. Uncertainty: +2 ft, -2 ft.

PPw X-ray data show a change from a mineral assemblage indicative of devitrification to zeolitized mineralogy at depths between 1744 and 1827.2 ft. Data indicate an increase in porosity at depths between 1730.9 and 1749 ft. Contact assigned midway between 1744 and 1749 ft. Uncertainty: +3 ft, -3 ft.

CFUn X-ray data indicate a change from a mineralogy dominated by zeolites to a mineralogy assemblage indicative of devitrification at depths between 2013.2 and 2070.2 ft. Data show a decrease in porosity at depths between 2069.6 and 2091.1 ft. Contact assigned midway between 2069.6 and 2070.2 ft. Uncertainty: 0 ft.

BFw	X-ray data show a change from a mineral assemblage indicative of devitrification to a mineralogy dominated by zeolites at depths between 2467.4 and 2548.4 ft. Contact assigned at the midpoint of the interval. Uncertainty: +41 ft, -41 ft.
CFMn1	Transition from ashflow to bedded tuff in lithologic log.
CFMn2	Transition from bedded tuff to ashflow in lithologic log.
TZZ	Based on the presence of a vitric mineralogy above PPw and the presence of a zeolitized interval within 6 ft of the base of PPw (as indicated by physical property data) contact is assigned at the base of PPw. Uncertainty: +6 ft.

Sources of information:

Lithologic log: Scott and Castellanos (1984, pp. 94-121)
Mineralogy: Vaniman et al (1984, pp. 6-8)
Bulk Properties: Schwartz (1983)

USW G-4

TCw	Transition from devitrified to vitric tuff in lithologic log.
PTn	Transition from vitric tuff to devitrified tuff in lithologic log.
TSw1	Contact assigned at the bottom of the lowermost ashflow of the Topopah Spring Member, which contains "common" lithophysae, based on the lithologic log.
TSw2	Transition from devitrified tuff to vitrophyre in lithologic log.
TSw3	Transition from vitrophyre to vitric ashflow in lithologic log.
CHn1	Transition from ashflow to basal bedded unit of the Tuffaceous Beds of the Calico Hills in lithologic log.
CHn2	Transition from bedded unit to ashflow in lithologic log.
CHn3	X-ray data indicate a change from a mineralogy dominated by zeolites to a mineral assemblage indicative of devitrification at depths between 1788 and 1794 ft. Contact assigned at the midpoint of the interval. Uncertainty: +2 ft, -2 ft.
PPw	X-ray data show a change from a mineral assemblage indicative of devitrification to a mineralogy dominated by zeolites at depths between 1952 and 1968 ft. Contact assigned at the midpoint of the interval. Uncertainty: +8 ft, -8 ft.

CFUn X-ray data indicate a change from a mineralogy dominated by zeolites to a mineral assemblage indicative of devitrification at depths between 2238 and 2263 ft. Contact assigned at 2258 ft, based on density log. Uncertainty: +5 ft, -20 ft.

BFw X-ray data indicate a change from a mineral assemblage indicative of devitrification to a mineralogy dominated by zeolites at depths between 2681 and 2716 ft. Contact assigned at 2682 ft based on density log. Uncertainty: +34 ft, -1 ft.

CFMn1 Transition from ashflow to bedded tuff in lithologic log.

CFMn2 Transition from bedded tuff to ashflow in lithologic log.

CFMn3 X-ray data indicate a change from a mineralogy dominated by zeolites to a mineral assemblage indicative of devitrification at depths between 2823 and 2840 ft. Contact assigned at 2828 ft, based on density log. Uncertainty: +12 ft, -5 ft.

TZZ Base of TSw3 is at 1345.4 ft depth, and X-ray data show zeolites present at a depth of 1381 ft. Core examination suggests assignment of the contact at a depth of 1363.5 ft. Uncertainty: +2 ft, -2 ft (core examination); +17 ft, -19 ft (X-ray data).

Sources of information:

Lithologic log: Spengler and Chornack (1984, pp. 62-77)
Mineralogy: Bish (1984)

USW H-1

TCw Transition from devitrified to vitric tuff in lithologic log.

CHn1 Transition from ashflow to basal bedded unit of the Tuffaceous Beds of the Calico Hills in lithologic log.

CHn2 Transition from bedded unit to ashflow in lithologic log.

CFMn1 Transition from ashflow to bedded tuff in lithologic log.

CFMn2 Transition from bedded tuff to ashflow in lithologic log.

Sources of information:

Lithologic log: Rush et al (1983, pp. 5-6)

USW H-3

TCw	Transition from devitrified to vitric tuff in lithologic log.
PTn	Contact assigned at top of interval containing vitrophyre fragments, as described in the lithologic log.
TSw2	Transition from devitrified tuff to vitrophyre in lithologic log.
TSw3	Transition from vitrophyre to vitric ashflow in lithologic log.
CHn1	Transition from ashflow to basal bedded unit of the Tuffaceous Beds of the Calico Hills in lithologic log.
CHn2	Transition from bedded unit to ashflow in lithologic log.
CHn3	Contact assigned at the base of the highest ashflow in the Prow Pass Member, based on descriptions in the lithologic log.
PPw	X-ray data show a change from a mineral assemblage indicative of devitrification to a mineralogy dominated by zeolites at depths between 1700 and 1800 ft. Contact is assigned at the base of the second highest ashflow in the Prow Pass Member, based on the lithologic log. Uncertainty: +90 ft, -10 ft.
CFUn	Contact assigned at the base of the second highest ashflow in the Bullfrog Member, based on the assumption that the partially welded ashflow is zeolitized but the underlying densely welded ashflow is not (descriptions from the lithologic log).
BFw	Contact assigned at the base of the second lowest ashflow in the Bullfrog Member, using the reverse of the reasoning used for Unit CFUn.
CFMn1	Transition from ashflow to bedded tuff in lithologic log.
CFMn2	Transition from bedded tuff to ashflow in lithologic log.
TZZ	Contact assigned at the base of Unit PPw, resulting from the descriptions in the lithologic log. Uncertainty: +90 ft, -10 ft.

Sources of information:

Lithologic log: Thordarson et al (1984, pp. 4-10)
Mineralogy: Levy (1984, p. 9)

USW H-4

TCw	Transition from devitrified to vitric tuff in lithologic log.
PTn	Transition from vitric tuff to devitrified tuff in lithologic log.
TSw2	Transition from devitrified tuff to vitrophyre in lithologic log.
TSw3	Transition from vitrophyre to vitric ashflow in lithologic log.
CHn1	Transition from ashflow to basal bedded unit of the Tuffaceous Beds of the Calico Hills in lithologic log.
CHn2	Transition from bedded unit to ashflow in lithologic log.
CHn3	Contact assigned at the base of the highest ashflow in the Prow Pass Member, based on descriptions in the lithologic log.
PPw	Transition from zeolitized tuff to devitrified tuff in lithologic log.
CFUn	Contact assigned at a depth of 2292 ft, based on density log. Uncertainty: +4 ft, -12 ft.
BFw	Contact assigned at a depth of 2581 ft, based on density log. Uncertainty: +23 ft, -23 ft.
CFMn1	Transition from ashflow to bedded tuff in log.
CFMn2	Transition from bedded tuff to ashflow in lithologic log.
CFMn3	Contact assigned at a depth of 2795 ft, based on density log. Uncertainty: +0 ft, -50 ft.
TRw	Contact assigned at a depth of 3207 ft, based on density log. Uncertainty: +0 ft, -10 ft.
TZZ	X-ray data indicate a change from glass to a mineralogy dominated by zeolites at depths between 1312 and 1420 ft. Contact assigned at a depth of 1316 ft, based on density log. Uncertainty: +108 ft, -4 ft.

Sources of information:

Lithologic log: Whitfield et al (1984, pp. 5-11)
Mineralogy: Levy (1984, p. 9)

USW H-5

TCw	Transition from devitrified to vitric tuff in lithologic log.
PTn	Transition from vitric tuff to devitrified tuff in lithologic log.
TSw2	Transition from devitrified tuff to vitrophyre in lithologic log.
TSw3	Transition from vitrophyre to vitric ashflow in lithogic log.
CHn1	Transition from ashflow to basal bedded unit of the Tuffaceous Beds of Calico Hills in lithologic log.
CHn2	Transition from bedded unit to ashflow in lithologic log.
CHn3	Contact assigned at a depth of 2015 ft, based on density log. Uncertainty: +7 ft, -4 ft.
PPw	Contact assigned at the base of the second lowest ashflow in the Prow Pass Member, based on the descriptions in the lithologic log.
CFUn	Contact assigned at a depth of 2345 ft, based on density log. Uncertainty: +7 ft, -4 ft.
BFw	Contact assigned at the base of the second lowest ashflow in the Bullfrog Member because of the descriptions in the lithologic log.
CFMn1	Transition from ashflow to bedded tuff in lithologic log.
CFMn2	Transition from bedded tuff to ashflow tuff in lithologic log.
CFMn3	Contact assigned at a depth of 2847 ft, based on density log. Uncertainty: +15 ft, -2 ft.
TRw	Contact assigned at a depth of 3144 ft, based on density log. Uncertainty: +0 ft, -14 ft.
TZZ	X-ray data indicate a change from glass to a mineral assemblage dominated by zeolites at depths between 1875 and 1917 ft. Contact is assigned at the midpoint of the interval. Uncertainty: +21 ft, -21 ft.

Sources of information:

Lithologic log: Bentley et al (1983, pp. 6-12)
Mineralogy: Levy (1984, p. 9)

USW H-6

TCw	Transition from devitrified to vitric tuff in lithologic log.
PTn	Transition from vitric tuff to devitrified tuff in lithologic log; an unquantified uncertainty is indicated in the log.
TSw2	Transition from devitrified tuff to vitrophyre in lithologic log.
TSw3	Transition from vitrophyre to vitric ashflow in lithologic log.
CHn1	Transition from ash flow to basal bedded unit of the Tuffaceous Beds of the Calico Hills in lithologic log.
CHn2	Transition from bedded unit to ashflow in lithologic log.
CHn3	Contact assigned at a depth of 1545 ft, based on density log. Uncertainty: +13 ft, -13 ft.
PPw	Contact assigned at a depth of 1720 ft, based on density log. Uncertainty: +2 ft, -13 ft.
CFUn	Contact assigned at a depth of 1806 ft, based on density log. Uncertainty: +6 ft, -6 ft.
BFw	Contact assigned at a depth of 2150 ft, based on density log. Uncertainty: +12 ft, -12 ft.
CFMn1	Transition from ashflow to bedded tuff in lithologic log.
CFMn2	Transition from bedded tuff to ashflow in lithologic log.
CFMn3	Contact assigned at a depth of 2352 ft, based on density log. Uncertainty: +6 ft, -6 ft.
TRw	Contact assigned at a depth of 2661 ft, based on density log. Uncertainty: +7 ft, -7 ft.
TZZ	Contact assigned at the base of Unit PPw, based on density log and description in the lithologic log of the lowest ashflow in the Prow Pass Member.

Sources of information:

Lithologic log: Craig et al (1983, pp. 5-12)

Table B-1
Data From UE-25a#1 Used to Generate Model
(E566350, N764900, 3934 ft)

Reference Stratigraphy Unit Designator	Mineralogy*	Unadjusted Elevation of Base of Unit (ft)	East-West Correction (ft)**		North-South Correction (ft)***		Vertical Correction (ft)		Adjusted Location		
			Deviation	Faulting	Deviation	Faulting	Deviation	Faulting	East-West	North-South	Elevation
UO		3904	-	-28	-	+3	-	-145	566322	764903	3759
TCw	d	3739	-1	-28	-	+3	-	-145	566321	764903	3594
PTn	v	3657	-3	-28	-	+3	-	-145	566319	764903	3512
TSw1	d	2858	-20	-28	-9	+3	-	-145	566302	764894	2713
TSw2	d	2672	-28	-28	-14	+3	+1	-145	566294	764889	2528
TSw3	v	2617	-31	-28	-15	+3	+1	-145	566291	764888	2473
CHn1	z	2145	-64	-28	-35	+3	+2	-145	566258	764868	2002
CHn2	z	2098	-67	-28	-38	+3	+2	-145	566255	764865	1955
CHn3	z	2089	-68	-28	-38	+3	+3	-145	566254	764865	1947
PPw	d	1921	-80	-28	-48	+3	+4	-145	566242	764855	1780
CFUn	z	1598	-107	-28	-65	+3	+6	-145	566215	764838	1459

*: d - devitrified; v - vitric; z - zeolitic
**: Positive is toward the east
***: Positive is toward the north

Table B-2
Data From UE-25b#1 Used to Generate Model
(E566416, N765244, 3939 ft)

Reference Stratigraphy Unit Designator	Mineralogy*	Unadjusted Elevation of Base of Unit (ft)	East-West Correction (ft)**		North-South Correction (ft)***		Vertical Correction (ft)		Adjusted Location		
			Deviation	Faulting	Deviation	Faulting	Deviation	Faulting	East-West	North-South	Elevation
UO		3789	-	-28	-	+3	-	-145	566388	765247	3644
TCw	d	3729	-1	-28	-1	+3	+1	-145	566387	765246	3585
PTn	v	3659	-2	-28	-1	+3	+1	-145	566386	765246	3515
TSw1	d	ND	ND	ND	ND	ND	ND	ND	ND	ND	ND
TSw2	d	2644	-38	-28	-	+3	+2	-145	566350	765247	2501
TSw3	v	2609	-39	-28	-	+3	+2	-145	566349	765247	2466
CHn1	v	2589	-38	-28	-	+3	+2	-145	566350	765247	2446
CHn1	z	2099	-53	-28	-5	+3	+2	-145	566335	765242	1956
CHn2	z	2070	-54	-28	-6	+3	+2	-145	566334	765241	1927
CHn3	z	2043	-55	-28	-6	+3	+2	-145	566333	765241	1900
PPw	d	1853	-65	-28	-8	+3	+1	-145	566323	765239	1709
CFUn	z	1543	-92	-28	-18	+3	+3	-145	566296	765229	1401
BFw	d	1152	-132	-28	-34	+3	+5	-145	566256	765213	1012
CFMn1	z	1086	-141	-28	-38	+3	+6	-145	566247	765209	947
CFMn2	z	1056	-146	-28	-39	+3	+6	-145	566242	765208	917
CFMn3	z	1017	-151	-28	-41	+3	+7	-145	566237	765206	879
TRw	d	615	-211	-28	-65	+3	+13	-145	566177	765182	483

*: d - devitrified; v - vitric; z - zeolitic
**: Positive is toward the east
***: Positive is toward the north
ND: Not distinguished in this drill hole

Table B-3
Data from USW G-1 Used to Generate Model
(E561000, N770500, 4349 ft)

Reference Stratigraphy Unit Designator	Mineralogy*	Unadjusted Elevation of Base of Unit (ft)	East-West Correction (ft)**		North-South Correction (ft)***		Vertical Correction (ft)		Adjusted Location		
			Deviation	Faulting	Deviation	Faulting	Deviation	Faulting	East-West	North-South	Elevation
UO		4289	-	-	-	-	-	-	561000	770500	4289
TCw	d	-Absent-									
PTn	v	4069	-	-	-2	-	-	-	561000	770498	4069
TSw1	d	3352	-1	-	-13	-	-	-	560999	770487	3352
TSw2	d	3062	-	-	-20	-	-	-	561000	770480	3062
TSw3	v	3007	-	-	-22	-	-	-	561000	770478	3007
CHn1	v	2956	-	-	-24	-	-	-	561000	770476	2956
CHn1	z	2613	-	-	-38	-	-	-	561000	770462	2613
CHn2	z	2548	-	-	-42	-	-	-	561000	770458	2548
CHn3	z	2481	-	-	-45	-	-	-	561000	770455	2481
PPw	d	2352	-	-	-53	-	-	-	561000	770447	2352
CFUn	z	2032	-	-	-75	-	-	-	561000	770425	2032
BFw	d	1806	-	-8	-93	+1	-	-30	560992	770408	1776
CFMn1	z	1747	-	-8	-99	+1	-	-30	560992	770402	1717
CFMn2	z	1710	-	-8	-102	+1	-	-30	560992	770399	1680
CFMn3	z	1595	-	-8	-114	+1	-	-30	560992	770387	1565
TRw	d	1322	-	-8	-144	+1	-	-30	560992	770357	1292

*: d - devitrified; v - vitric; z - zeolitic
**: Positive is toward the east
***: Positive is toward the north

Table B-4
Data from USW G-2 Used to Generate Model
(E560504, N778824, 5098 ft)

Reference Stratigraphy Unit Designator	Mineralogy*	Unadjusted Elevation of Base of Unit (ft)	East-West Correction (ft)**		North-South Correction (ft)***		Vertical Correction (ft)		Adjusted Location		
			Deviation	Faulting	Deviation	Faulting	Deviation	Faulting	East-West	North-South	Elevation
TCw	d	4878	+5	-	+1	-	-	-	560509	778825	4878
PTn	v	4327	+15	-	-3	-	-	-	560519	778821	4327
TSw1	d	3605	+15	-	-15	-	-	-	560519	778809	3605
TSw2	d	3464	+10	-	-19	-	-	-	560514	778805	3464
TSw3	v	3429	+9	-	-20	-	+1	-	560513	778804	3430
CHn1	v	3421	+9	-	-21	-	+1	-	560513	778803	3422
CHn1	z	2394	-37	-	-46	-	+3	-	560467	778778	2397
CHn2	z	Absent due to faulting							560467	778778	2250
CHn3	z	2376	-37	-60	-48	-	+2	-224	560407	778776	2154
PPw	d	2046	-52	-60	-54	-	+2	-224	560392	778770	1824
CFUn	z	1821	-65	-60	-56	-	+3	-224	560379	778768	1600
BFw	d	1659	-75	-60	-56	-	+3	-224	560369	778768	1438
CFMn1	z	1595	-78	-60	-57	-	+3	-224	560366	778767	1374
CFMn2	z	1524	-82	-60	-58	-	+3	-224	560362	778766	1303
CFMn3	z	1519	-84	-60	-57	-	+3	-224	560360	778767	1298
TRw	d	1187	-101	-60	-58	-	+4	-224	560343	778766	967

*: d - devitrified; v - vitric; z - zeolitic
**: Positive is toward the east
***: Positive is toward the north

Table B-5
Data from USW GU-3 Used to Generate Model
(E558501, N752690, 4857 ft)

Reference Stratigraphy Unit Designator	Mineralogy*	Unadjusted Elevation of Base of Unit (ft)	East-West Correction (ft)**		North-South Correction (ft)***		Vertical Correction (ft)		Adjusted Location		
			Deviation	Faulting	Deviation	Faulting	Deviation	Faulting	East-West	North-South	Elevation
TCw	d	4514	+3	-	-6	-	-	-	558504	752684	4513****
PTn	v	4427	+2	-	-8	-	-	-	558503	752682	4427
TSw1	d	4167	+2	-	-14	-	-	-	558503	752676	4167
TSw2	d	3670	-1	-	-29	-	-	-	558500	752661	3670
TSw3	v	3588	-1	-	-33	-	+1	-	558500	752657	3589
CHn1	v	3350	-4	-	-47	-	+2	-	558497	752643	3352
CHn2	v	3297	-5	-	-50	-	+2	-	558496	752640	3299
CHn3	v	3256	-6	-	-52	-	+2	-	558495	752638	3258
PPw	d	3111	-11	-	-60	-	-	-	558490	752630	3111
CFUn	z	2787	-26	-	-77	-	+2	-	558475	752613	2789
BFw	d	2349	-53	-	-104	-	+4	-	558448	752586	2353
CFMn1	z	2240	NA	-	NA	-	NA	-	558448	752586	2244
CFMn2	z	2220	NA	-	NA	-	NA	-	558448	752586	2224

*: d - devitrified; v - vitric; z - zeolitic
**: Positive is toward the east
***: Positive is toward the north
****: Input data for I-A-2 was 4514
NA: Not available; assumed to be the same as that for the deepest unit above

Table B-6
Data from USW G-4 Used to Generate Model
(E563082, N765807, 4165 ft)

Reference Stratigraphy Unit Designator	Mineralogy*	Unadjusted Elevation of Base of Unit (ft)	East-West Correction (ft)**		North-South Correction (ft)***		Vertical Correction (ft)		Adjusted Location		
			Deviation	Faulting	Deviation	Faulting	Deviation	Faulting	East-West	North-South	Elevation
UO		4135	-	-7	-	+1	-	-65	563075	765808	4070
TCw	d	4047	-	-7	-	+1	-	-65	563075	765808	3982
PTn	v	3922	-1	-7	-1	+1	-	-65	563074	765807	3857
TSw1	d	3495	-6	-7	-4	+1	-	-65	563069	765804	3430
TSw2	d	2872	-36	-7	-41	+1	+2	-65	563039	765767	2809
TSw3	v	2820	-40	-7	-46	+1	+2	-65	563035	765762	2757
CHn1	v	2802	-41	-7	-47	+1	+3	-65	563034	765761	2743****
CHn1	z	2460	-70	-7	-71	+1	+4	-65	563005	765737	2399
CHn2	z	2404	-75	-7	-74	+1	+5	-65	563000	765734	2344
CHn3	z	2373	-78	-7	-76	+1	+5	-65	562997	765732	2313
PPw	d	2205	-94	-7	-87	+1	+6	-65	562981	765721	2146
CFUn	z	1907	-124	-7	-105	+1	+8	-65	562951	765703	1850
BFw	d	1483	-176	-7	-125	+1	+12	-65	562899	765683	1430
CFMn1	z	1432	-183	-7	-126	+1	+13	-65	562892	765682	1380
CFMn2	z	1409	-186	-7	-127	+1	+13	-65	562889	765681	1357
CFMn3	z	1337	-196	-7	-132	+1	+14	-65	562879	765676	1286

*: d - devitrified; v - vitric; z - zeolitic
**: Positive is toward the east
***: Positive is toward the north
****: Input data for IV-A was 2740

Table B-7
Data from USW H-1 Used to Generate Model
(E562388, N770254, 4272 ft)

Reference Stratigraphy Unit Designator	Mineralogy*	Unadjusted Elevation of Base of Unit (ft)	East-West Correction (ft)**		North-South Correction (ft)***		Vertical Correction (ft)		Adjusted Location		
			Deviation	Faulting	Deviation	Faulting	Deviation	Faulting	East-West	North-South	Elevation
TCw	d	4183	-	-8	-	+1	-	-30	562380	770255	4153
---No thermal/mechanical units distinguished in this interval---											
CHn1	z	2471	+4	-8	-12	+1	+1	-30	562384	770243	2442
CHn2	z	2415	+2	-8	-14	+1	+1	-30	562382	770241	2386
---No thermal/mechanical units distinguished in this interval---											
CFMn1	z	1582	-19	-8	-34	+1	+1	-30	562361	770221	1553
CFMn2	z	1542	-19	-8	-34	+1	+1	-30	562361	770221	1513

Scott and Bank (1984) indicate that UO (QTac) is present but no thickness is given in lithologic log.
*: d - devitrified; v - vitric; z - zeolitic
**: Positive is toward the east
***: Positive is toward the north

Table B-8
Data from USW H-3 Used to Generate Model
(E558452, N756542, 4866 ft)

Reference Stratigraphy Unit Designator	Mineralogy*	Unadjusted Elevation of Base of Unit (ft)	East-West Correction (ft)**		North-South Correction (ft)***		Vertical Correction (ft)		Adjusted Location		
			Deviation	Faulting	Deviation	Faulting	Deviation	Faulting	East-West	North-South	Elevation
TCw	d	4516	-2	-	-2	-	-	-	558450	756540	4516
PTn	v	4416	-2	-	-2	-	-	-	558450	756540	4416
TSw1	d	ND	ND	ND	ND	ND	ND	ND	ND	ND	ND
TSw2	d	3672	-3	-	+3	-	-	-	558449	756545	3672
TSw3	v	3614	-4	-	+3	-	-	-	558448	756545	3614
CHn1	v	3429	-7	-	+5	-	-	-	558445	756547	3429
CHn2	v	3379	-7	-	+5	-	-	-	558445	756547	3379
CHn3	v	3162	-9	-	+6	-	-	-	558443	756548	3162
PPw	d	3156	-10	-	+7	-	-	-	558442	756549	3156
CFUn	z	2866	-13	-	+8	-	-	-	558439	756550	2866
BFw	d	2543	-19	-	+10	-	-	-	558433	756552	2543
CFMn1	z	2417	-22	-	+11	-	-	-	558430	756553	2417
CFMn2	z	2389	-23	-	+11	-	-	-	558429	756553	2389

*: d - devitrified; v - vitric; z - zeolitic
**: Positive is toward the east
***: Positive is toward the north
ND: Not distinguished in this drill hole

Table B-9
Data From USW H-4 Used to Generate Model
(E563911, N761644, 4097 ft)

Reference Stratigraphy Unit Designator	Mineralogy*	Unadjusted Elevation of Base of Unit (ft)	East-West Correction (ft)**		North-South Correction (ft)***		Vertical Correction (ft)		Adjusted Location		
			Deviation	Faulting	Deviation	Faulting	Deviation	Faulting	East-West	North-South	Elevation
TCw	d	3923	+2	-15	-1	+1	-	-140	563898	761644	3783
PTn	v	3845	+2	-15	-1	+1	-	-140	563898	761644	3705
TSw1	d	ND	ND	ND	ND	ND	ND	ND	ND	ND	ND
TSw2	d	2912	+9	-15	-2	+1	-	-140	563905	761643	2772
TSw3	v	2880	+8	-15	-2	+1	-	-140	563904	761643	2740
CHn1	v	2781	+6	-15	-1	+1	-	-140	563902	761644	2641
CHn1	z	2522	-	-15	+1	+1	-	-140	563896	761646	2382
CHn2	z	2470	-	-15	+1	+1	-	-140	563896	761646	2330
CHn3	z	2457	-1	-15	+1	+1	-	-140	563895	761646	2317
PPw	d	2337	-3	-15	+2	+1	-	-140	563893	761647	2197
CFUn	z	1805	-12	-15	+6	+1	-	-140	563884	761651	1665
BFw	d	1516	-16	-15	+7	+1	-	-140	563880	761652	1376
CFMn1	z	1453	-16	-15	+7	+1	-	-140	563880	761652	1313
CFMn2	z	1433	-16	-15	+8	+1	-	-140	563880	761653	1293
CFMn3	z	1302	-18	-15	+9	+1	-	-140	563878	761654	1162
TRw	d	890	-24	-15	+12	+1	-	-140	563872	761657	750

Scott and Bank (1984) indicate that UO (QTac) is present but no thickness is given in lithologic log.
*: d - devitrified; v - vitric; z - zeolitic
**: Positive is toward the east
***: Positive is toward the north
ND: Not distinguished in this drill hole

• Work performed after the writing of this report indicates that the vertical correction for faulting should be approximately -100 ft.

Table B-10
Data From USW H-5 Used to Generate Model
(E558909, N766634, 4851 ft)

Reference Stratigraphy Unit Designator	Mineralogy*	Unadjusted Elevation of Base of Unit (ft)	East-West Correction (ft)**		North-South Correction (ft)***		Vertical Correction (ft)		Adjusted Location		
			Deviation	Faulting	Deviation	Faulting	Deviation	Faulting	East-West	North-South	Elevation
TCw	d	4441	+3	–	-1	–	–	–	558912	766633	4441
PTn	v	4281	+4	–	-4	–	–	–	558913	766630	4281
TSw1	d	ND	ND	ND	ND	ND	ND	ND	ND	ND	ND
TSw2	d	3269	-11	–	-10	–	–	–	558898	766624	3269
TSw3	v	3196	-11	–	-10	–	–	–	558898	766624	3196
CHn1	v	2971	-14	–	-10	–	–	–	558895	766624	2971
CHn2	v	2955	-14	–	-10	–	–	–	558895	766624	2955
CHn2	z	2906	-15	–	-9	–	–	–	558894	766625	2906
CHn3	z	2836	-16	–	-9	–	–	–	558893	766625	2836
PPw	d	2726	-17	–	-9	–	–	–	558892	766625	2726
CFUn	z	2506	-19	–	-9	–	–	–	558890	766625	2506
BFw	d	2141	-22	–	-9	–	–	–	558887	766625	2141
CFMn1	z	2138	-22	–	-9	–	–	–	558887	766625	2138
CFMn2	z	2109	-22	–	-9	–	–	–	558887	766625	2109
CFMn3	z	2004	-23	–	-9	–	–	–	558886	766625	2004
TRw	d	1707	-26	–	-11	–	–	–	558883	766623	1707

*: d - devitrified; v - vitric; z - zeolitic
**: Positive is toward the east
***: Positive is toward the north
ND: Not distinguished in this drill hole

Table B-11
Data From USW H-6 Used to Generate Model
(E554075, N763299, 4271 ft)

Reference Stratigraphy Unit Designator	Mineralogy*	Unadjusted Elevation of Base of Unit (ft)	East-West Correction (ft)**		North-South Correction (ft)***		Vertical Correction (ft)		Adjusted Location		
			Deviation	Faulting	Deviation	Faulting	Deviation	Faulting	East-West	North-South	Elevation
UO		4241	-	+109	-	-40	-	+600	554184	763259	4841
TCw	d	4081	-2	+109	-	-40	-	+600	554182	763259	4681
PTn	v	3939	-4	+109	-	-40	-	+600	554180	763259	4539
TSw1	d	ND	ND	ND	ND	ND	ND	ND	ND	ND	ND
TSw2	d	3054	-16	+109	-	-40	-	+600	554168	763259	3654
TSw3	v	2964	-17	+109	-	-40	-	+600	554167	763259	3564
CHn1	v	2813	-19	+109	+1	-40	-	+600	554165	763260	3413
CHn2	v	2767	-20	+109	+1	-40	-	+600	554164	763260	3367
CHn3	v	2726	-20	+109	+1	-40	-	+600	554164	763260	3326
PPw	d	2551	-23	+109	+1	-40	-	+600	554161	763260	3151
CFUn	z	2465	-24	+109	+1	-40	-	+600	554160	763260	3065
BFw	d	2121	-28	+109	+1	-40	-	+600	554156	763260	2721
CFMn1	z	2046	-29	+109	+1	-40	-	+600	554155	763260	2646
CFMn2	z	2016	-30	+109	+1	-40	-	+600	554154	763260	2616
CFMn3	z	1919	-31	+109	+1	-40	-	+600	544153	763260	2519
TRw	d	1610	-35	+109	+1	-40	-	+600	544149	763260	2210

*: d - devitrified; v - vitric; z - zeolitic
**: Positive is toward the east
***: Positive is toward the north
ND: Not distinguished in this drill hole

Table B-12
Data From Other Drill Holes and Surface Outcrops Used to Generate Model

Reference Stratigraphy Unit Designator	Mineralogy*	Unadjusted Elevation of Base of Unit (ft)	East-West Correction (ft)**		North-South Correction (ft)***		Vertical Correction (ft)		Adjusted Location		
			Deviation	Faulting	Deviation	Faulting	Deviation	Faulting	East-West	North-South	Elevation
UE-25a#4 (E564472, N767972, 4101 ft)											
UO		4071	–	-1	–	–	–	-5	564472	767972	4066
TCw	d	3980	–	-1	–	–	–	-5	564471	767972	3975
PTn	v	3781	–	-1	–	–	–	-5	564471	767972	3776
UE-25a#5 (E564755, N766956, 4057 ft)											
UO		3967	–	-3	–	–	–	-30	564752	766956	3937
TCw	d	3929	–	-3	–	–	–	-30	564752	766956	3899
PTn	v	3778	–	-3	–	–	–	-30	564752	766956	3748
UE-25a#6 (E564501, N765899, 4052 ft)											
UO		4032	–	-6	–	–	–	-55	564495	765899	3977
TCw	d	3929	–	-6	–	–	–	-55	564495	765899	3874
PTn	v	3806	–	-6	–	–	–	-55	564495	765899	3751
UE-25a#7 (E565469, N766250, 4005 ft)											
UO		3867	–	-5	–	–	–	-45	565464	766250	3822
TCw	d	3849****	-59	-5	-48	–	–	-45	565405	766202	3804
PTn	v	3728****	-105	-5	-85	–	–	-45	565359	766165	3683
S1 (E556958, N760704, 4300 ft)											
TSw1	d	4300	–	–	–	–	–	–	556958	760704	4300
S2 (E557481, N755406, 4300 ft)											
TSw1	d	4300	–	–	–	–	–	–	557481	755406	4300

*: d – devitrified; v – vitric
**: Positive is toward the east
***: Positive is toward the north
****: UE-25a#7 is slanted at 26° to the vertical. Vertical deviations were calculated by Spengler and Rosenbaum (1980). The elevations given here are the true, or adjusted, elevations.

Table B-13

Gyroscopic Surveys Used in Hole Deviation Calculations

Drill Hole	Survey Date
UE-25a#1	08/26/78
UE-25b#1	08/03/81
USW G-1	04/29/80
USW G-2	10/13/81
USW GU-3	05/18/82
USW G-4	11/07/82
USW H-1	11/22/80
USW H-3	02/03/82
USW H-4	04/30/82
USW H-5	06/23/82

Table B-14
Apparent Dips and Offsets of Faults

$\tan \rho = \tan \delta \sin \alpha$

where ρ = apparent dip(°)
δ = true dip(°)
α = angle between strike of fault and section line

Fault*	δ	α	ρ	Assumed Displacement (ft)
L1	75	93	75	200
L2	75	111	74	80
L3	75	82	75	300
L4	84	78	84	65
L5	75	90	75	40
L6	75	90	75	40
M1	90	150	89	0
M2	90	140	95	0
M3	62	8	14.5	224
N1	75	121	73	20
N2	75	140	67	0
N3	75	140	67	0
N4	75	138	68	0
N5	75	138	68	0
N6	82	161	67	125
N7	90	115	90	0
N8	75	53	71	10
N9	75	53	71	10
N10	75	95	75	10
N11	75	90	75	10
N12	75	125	72	10
P1	73	115	71	41
P2	75	68	74	200
P3	75	74	74	50
P4	75	74	74	25
P5	75	50	73	300
P6	82	50	79	130
P7	79	54	76	70
P8	77	70	76	20
P9	75	78	75	20
P10	77	78	77	50

*See Figures 4-8 for location.

NOTE: In most cases, true dips assumed to be 75° for normal faults and 90° for strike-slip faults. Dips different from those were used to be consistent with Scott and Bonk (1984).

APPENDIX C
CORRELATION BETWEEN FORMER UNIT DESIGNATORS AND UNIT DESIGNATORS ESTABLISHED IN THIS REPORT

Reference Stratigraphy Unit Name (Designator)	Former Unit Designator*
Undifferentiated Overburden (UO)	IA1
Tiva Canyon welded (TCw)	IA2
Upper Paintbrush Tuff nonwelded (PTn)	IB
Topopah Spring welded lithophysae-rich (TSw1)	IIL
Topopah Spring welded lithophysae-poor (TSw2)	IINL
Topopah Spring welded vitrophyre (TSw3)	III
Calico Hills and Lower Paintbrush nonwelded (CHn1)	IVA
Calico Hills and Lower Paintbrush nonwelded (CHn2)	IVB
Calico Hills and Lower Paintbrush nonwelded (CHn3)	IVC
Prow Pass welded (PPw)	V
Upper Crater Flat nonwelded (CFUn)	VI
Bullfrog welded (BFw)	VII
Middle Crater Flat nonwelded (CFMn1)	VIIIA
Middle Crater Flat nonwelded (CFMn2)	VIIIB
Middle Crater Flat nonwelded (CFMn3)	VIIIC
Tram welded (TRw)	IX

* SNL memo from Nimick, F. B. to Distribution, 6/5/84, "Thermal/Mechanical Units at Yucca Mountain."

DISTRIBUTION LIST

B. C. Rusche (RW-1)
Director
Office of Civilian Radioactive
Waste Management
U.S. Department of Energy
Forrestal Building
Washington, DC 20585

Ralph Stein (RW-23)
Office of Geologic Repositories
U.S. Department of Energy
Forrestal Building
Washington, DC 20585

J. J. Fiore, (RW-22)
Program Management Division
Office of Geologic Repositories
U.S. Department of Energy
Forrestal Building
Washington, DC 20585

M. W. Frei (RW-23)
Engineering & Licensing Division
Office of Geologic Repositories
U.S. Department of Energy
Forrestal Building
Washington, DC 20585

E. S. Burton (RW-25)
Siting Division
Office of Geologic Repositories
U.S. Department of Energy
Forrestal Building
Washington, D.C. 20585

C. R. Cooley (RW-24)
Geosciences & Technology Division
Office of Geologic Repositories
U.S. Department of Energy
Forrestal Building
Washington, DC 20585

V. J. Cassella (RW-22)
Office of Geologic Repositories
U.S. Department of Energy
Forrestal Building
Washington, DC 20585

T. P. Longo (RW-25)
Program Management Division
Office of Geologic Repositories
U.S. Department of Energy
Forrestal Building
Washington, DC 20585

Cy Klingsberg (RW-24)
Geosciences and Technology Division
Office of Geologic Repositories
U. S. Department of Energy
Forrestal Building
Washington, DC 20585

B. G. Gale (RW-25)
Siting Division
Office of Geologic Repositories
U.S. Department of Energy
Forrestal Building
Washington, D.C. 20585

R. J. Blaney (RW-22)
Program Management Division
Office of Geologic Repositories
U.S. Department of Energy
Forrestal Building
Washington, DC 20585

R. W. Gale (RW-40)
Office of Policy, Integration, and
Outreach
U.S. Department of Energy
Forrestal Building
Washington, D.C. 20585

J. E. Shaheen (RW-44)
Outreach Programs
Office of Policy, Integration and
Outreach
U.S. Department of Energy
Forrestal Building
Washington, DC 20585

J. O. Neff, Manager
Salt Repository Project Office
U.S. Department of Energy
505 King Avenue
Columbus, OH 43201

D. C. Newton (RW-23)
Engineering & Licensing Division
Office of Geologic Repositories
U.S. Department of Energy
Forrestal Building
Washington, DC 20585

O. L. Olson, Manager
Basalt Waste Isolation Project Office
U.S. Department of Energy
Richland Operations Office
Post Office Box 550
Richland, WA 99352

D. L. Vieth, Director (4)
Waste Management Project Office
U.S. Department of Energy
Post Office Box 14100
Las Vegas, NV 89114

D. F. Miller, Director
Office of Public Affairs
U.S. Department of Energy
Post Office Box 14100
Las Vegas, NV 89114

D. A. Nowack (12)
Office of Public Affairs
U.S. Department of Energy
Post Office Box 14100
Las Vegas, NV 89114

B. W. Church, Director
Health Physics Division
U.S. Department of Energy
Post Office Box 14100
Las Vegas, NV 89114

Chief, Repository Projects Branch
Division of Waste Management
U.S. Nuclear Regulatory Commission
Washington, D.C. 20555

Document Control Center
Division of Waste Management
U.S. Nuclear Regulatory Commission
Washington, D.C. 20555

S. A. Mann, Manager
Crystalline Rock Project Office
U.S. Department of Energy
9800 South Cass Avenue
Argonne, IL 60439

K. Street, Jr.
Lawrence Livermore National
Laboratory
Post Office Box 808
Mail Stop L-209
Livermore, CA 94550

L. D. Ramspott (3)
Technical Project Officer for NNWSI
Lawrence Livermore National
Laboratory
P.O. Box 808
Mail Stop L-204
Livermore, CA 94550

W. J. Purcell (RW-20)
Office of Geologic Repositories
U.S. Department of Energy
Forrestal Building
Washington, DC 20585

D. T. Oakley (4)
Technical Project Officer for NNWSI
Los Alamos National Laboratory
P.O. Box 1663
Mail Stop F-619
Los Alamos, NM 87545

W. W. Dudley, Jr. (3)
Technical Project Officer for NNWSI
U.S. Geological Survey
Post Office Box 25046
418 Federal Center
Denver, CO 80225

NTS Section Leader
Repository Project Branch
Division of Waste Management
U.S. Nuclear Regulatory Commission
Washington, D.C. 20555

V. M. Glanzman
U.S. Geological Survey
Post Office Box 25046
913 Federal Center
Denver, CO 80225

P. T. Prestholt
NRC Site Representative
1050 East Flamingo Road
Suite 319
Las Vegas, NV 89109

J. B. Wright
Technical Project Officer for NNWSI
Westinghouse Electric Corporation
Waste Technology Services Division
Nevada Operations
Post Office Box 708
Mail Stop 703
Mercury, NV 89023

M. E. Spaeth
Technical Project Officer for NNWSI
Science Applications
International, Corporation
2769 South Highland Drive
Las Vegas, NV 89109

ONWI Library
Battelle Columbus Laboratory
Office of Nuclear Waste Isolation
505 King Avenue
Columbus, OH 43201

SAIC-T&MSS Library (2)
Science Applications
International, Corporation
2950 South Highland Drive
Las Vegas, NV 89109

W. M. Hewitt, Program Manager
Roy F. Weston, Inc.
2301 Research Blvd., 3rd Floor
Rockville, MD 20850

W. S. Twenhofel, Consultant
Science Applications
International, Corp.
820 Estes Street
Lakewood, CO 80215

H. D. Cunningham
General Manager
Reynolds Electrical &
Engineering Co., Inc.
Post Office Box 14400
Mail Stop 555
Las Vegas, NV 89114

A. E. Gurrola
General Manager
Energy Support Division
Holmes & Narver, Inc.
Post Office Box 14340
Las Vegas, NV 89114

T. Hay, Executive Assistant
Office of the Governor
State of Nevada
Capitol Complex
Carson City, NV 89710

J. A. Cross, Manager
Las Vegas Branch
Fenix & Scisson, Inc.
Post Office Box 15408
Las Vegas, NV 89114

R. R. Loux, Jr., Director (3)
Nuclear Waste Project Office
State of Nevada
Capitol Complex
Carson City, NV 89710

Neal Duncan (RW-44)
Office of Policy, Integration, and
Outreach
U.S. Department of Energy
Forrestal Building
Washington, DC 20585

C. H. Johnson, Technical
Program Manager
Nuclear Waste Project Office
State of Nevada
Capitol Complex
Carson City, NV 89710

John Fordham
Desert Research Institute
Water Resources Center
Post Office Box 60220
Reno, NV 89506

Dr. Martin Mifflin
Desert Research Institute
Water Resources Center
Suite 1
2505 Chandler Avenue
Las Vegas, NV 89120

Department of Comprehensive
Planning
Clark County
225 Bridger Avenue, 7th Floor
Las Vegas, NV 89155

Planning Department
Nye County
Post Office Box 153
Tonopah, NV 89049

Lincoln County Commission
Lincoln County
Post Office Box 90
Pioche, NV 89043

Economic Development
Department
City of Las Vegas
400 East Stewart Avenue
Las Vegas, NV 89101

Community Planning and
Development
City of North Las Vegas
Post Office Box 4086
North Las Vegas, NV 89030

Director of Community
Planning
City of Boulder City
Post Office Box 367
Boulder City, NV 89005

City Manager
City of Henderson
Henderson, NV 89015

Commission of the
European Communities
200 Rue de la Loi
B-1049 Brussels
BELGIUM

N. A. Norman
Project Manager
Bechtel National Inc.
P. O. Box 3965
San Francisco, CA 94119

Technical Information Center
Roy F. Weston, Inc.
2301 Research Boulevard,
Third Floor
Rockville, MD 20850

Flo Butler
Los Alamos Technical Associates
1650 Trinity Drive
Los Alamos, New Mexico 87544

R. Harig
Parsons Brinkerhoff Quade &
Douglas, Inc.
1625 Van Ness Ave.
San Francisco, CA 94109-3678

Timothy G. Barbour
Science Applications
International Corporation
1626 Cole Boulevard, Suite 270
Golden, CO 80401

Dr. Madan M. Singh, President
Engineers International, Inc.
98 East Naperville Road
Westmont, IL 60559-1595

6300 R. W. Lynch
6310 T. O. Hunter
6310 NNWSICF
6311 L. W. Scully
6311 L. Perrine (2)
6312 F. W. Bingham
6313 T. E. Blejwas
6313 F. B. Nimick (6)
6314 J. R. Tillerson
6332 WMT Library (20)

6315 S. Sinnock
6315 D. L. South
6315 B. C. Whittet
6315 R. L. Williams
6430 N. R. Ortiz
3141 C. M. Ostrander (5)
3151 W. L. Garner (3)
8024 M. A. Pound
DOE/TIC (28)
(3154-3, C. H. Dalin)